Appendix A
Body Vehicle Design Process

The purpose of this appendix is to provide the reader with an overview of product development technology and, in particular, of the role that computers play in it. To keep the size of this appendix within reasonable limits, our attention is concentrated on the car body only.

The reason for this choice is that the car body has some peculiar aspects and features that make it different from that of the other car subsystems, since the body is designed keeping in mind not only its technical characteristics and production technologies, but also the aesthetic characteristics of its '*style*', which plays a fundamental role in determining the commercial success of a car.

From a technical standpoint, a conventional steel body includes the body shell and trimming which are primarily made by thin-wall elements, whose external surface performs usually aesthetic functions; this fact alone justifies peculiar engineering techniques. These thin sheet elements of complex shape required the development of particular representation rules, that are different from those used for mechanical components (engine, transmission, suspensions, etc.), and that are limited to a few views and sections, aimed to keep the representation as simple as possible.

A further specific characteristic is related to the high capital investments needed to mass produce the vehicle body, with respect to its relatively short production life, usually limited to a few years. The body shell and trimming are totally revised at each new model launch, i.e. every $5 \div 7$ years on average, and this contrasts with what happens with many other components, invisible to the customer, that may be reused with only incremental improvements on next generation models.

This short life may be justified by the accepted tradition of transmitting the image of new product contents through a new shape, which is supposed to correspond better to the aesthetic tastes and style trends of the moment. The simultaneous needs for careful management of costs and cash flows for new investments on one hand, and for developing aesthetic forms consistent with the customer demand at the time of the commercial launch on the other, result in a strong pressure to shorten the time allocated to development. Although this requirement is shared also by other car components, it is a critical issue when dealing with the car body.

G. Genta et al., *The Motor Car*, Mechanical Engineering Series,
DOI: 10.1007/978-94-007-8552-6, © Springer Science+Business Media Dordrecht 2014

When considering body drawings, it should be remembered that they have different applications; they provide not only the description of parts to be manufactured but they are also the starting point for the development of other drawings that are just as important. With respect to a body shell stamped panel drawing, for example, the following items must be mutually consistent:

- The stamp set for production;
- The positioning and fixing tools for welding with the neighboring parts;
- The characteristics of the working robots for painting and assembling (usually applied for many model generations);
- The spare parts catalogues;
- The disassembling and assembling schemes for servicing and repairing.

The development of any of these items also includes activities which rely on body drawings, often including tests on actual or virtual prototypes. The latter are based on mathematical models that describe completely the geometry of the relevant components, to allow Finite Elements (FE) analysis or the construction of a Digital Mock-up (DMU) used to verify the geometrical compatibility between parts or to verify their kinematic behavior (e.g.: doors opening, wiper motion, side glasses opening, etc.).

A.1 Typical Activity Planning

Body drawings should be available early enough with respect to the start of production to enable all related activities to be performed. The project has thus to be organized is such a way that many activities can be performed in parallel and to accomplish this a minimum of information needed for performing each of these activities must be determined.

This so-called *simultaneous engineering* or *concurrent engineering* provides a means for organizing each elementary operation so that the results needed to initiate the successive operations with a minimum delay are produced. For instance, to start the design of a stamp or a positioning tool, it may be sufficient to determine the overall dimensions of the steel sheet rather than the details of its aesthetic shape; therefore tool drafting can be started before the body shell panel it will produce has been defined in detail. This way of organizing activities increases considerably the number of modifications to be introduced, either for completing drawings with additional detail, or for correcting mistakes that arise due to the lack of information available at the moment when the design was performed.

Correspondingly, the rate of modification becomes just as important as the drafting speed; in addition, the knowledge and know-how of those involved in the development process, and of those who perform subsequent activities, become critical factors for success. Consequently each of those involved in the process must aim for *final* customer satisfaction while effectively working also for an *internal* client who

will apply the results to other equally important activities from the perspective of production or commercialisation.

In the case of the body, organization of the development work is further complicated by the fact that each design engineer is not only the supplier to an internal client but is, at the same time, the customer of activities performed by designers developing the aesthetic shapes; actually, body engineering must be performed in parallel with style development.

Today an overall development time of about 24 months, from the style model choice to the start of production, represents the best performance achieved by major car manufacturers, although this is only possible thanks to the wide-ranging application of computers, regularly used for:

- Computer Aided Styling (CAS) applied to develop visible shapes,
- Computer Aided Drafting (CAD) applied to engineering activities related to final product or production tools,
- Computer Aided Manufacturing (CAM) applied to the design of some aspects of the production process,
- Digital Mock-Up (DMU) applied to represent complex assemblies for virtual testing or to develop production and assembly plant layout.

Computers not only reduced the time needed for drafting and for the implementation of modifications, but also made it possible to set up a unique data base that enables all the operations needed to keep product development aligned and updated.

The outside surface of a body panel, the result of the body style development, a part of the component drawings, stamp drawings, etc. may be in common, avoiding replication for different working environments and the risk of errors and delays.

The development process may be outlined as in Fig. A.1. The scheme demonstrates that a high project development speed (here engineering activities are divided in planning and engineering) can be justified by the existence of a phase, here termed

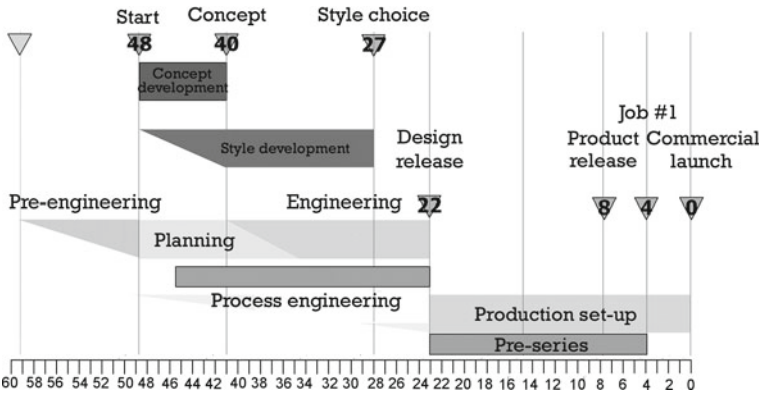

Fig. A.1 The logical scheme of the main phases of the development process, with specific reference to the body. The time scale, at the *bottom*, is measured in months from the commercial launch and the elapsed time is highlighted with respect to the major milestones (from Morello et al. 2011)

pre-engineering (or *shelf-engineering*), where alternative solutions are studied and validated experimentally, without a real finalization; these activities contribute to filling an ideal shelf where good ideas are stored, ready for future application.

The *concept* development phase, or feasibility study, is performed with the cooperation of engineers, marketing experts and stylists, who define a product specification (concept) by examining alternative solutions in parallel; this concept specification must simultaneously satisfy customer's aesthetic and functional expectations and achieve technical and economical feasibility.

Manufacturing of prototypes is started at almost the same time as engineering activities; consequently, prototypes relate to partial aspects only, allowing design features to be validated one at a time. Only at the end will prototypes similar to the final product be available to be used for design approval (or design release), to certify that each specification defined by the concept has been satisfied.

The so-called *pre-series* are other prototypes that, as opposed to the first ones, are built using mass production tools and plants; the positive conclusion of their tests is used for product approval (product release), i.e. providing certification that the production means and organization are adequate to obtain a product complying with specifications.

The *Job #1* vehicle is the first that can be delivered to final customers.

During the time elapsed between concept definition to product definition (from 40 to 22 months before the commercial launch) many activities are performed in parallel such as planning, engineering, style definition, planning and development of stamping, welding and assembling processes, economical evaluation and optimization, in addition to the manufacturing of prototypes that are increasingly complete and closer to the final product.

Many activities that, logically, would be executed in sequence are instead performed in parallel and, as a consequence, are based upon provisional and continually changing information. This organization of activities, apparently nonlogical, can provide advantages in term of cost and time assuming that design tools, in this case CAS, CAD and CAM, enable rapid modification and reutilizing of models for different purposes.

This procedure enables a product solution consistent with production processes, that will not require major changes during the following industrialization phase, to be developed 22 months before the commercial launch; it is therefore possible to start building production tools in time for validation eight months before commercial launch at the supplier's premises. Subsequently the production tools are transferred to the plant of the car manufacturer in order to initiate producing pre-series vehicles and accumulate the necessary numbers for commercial launch.

The advantages of CAD in terms of shortening the time for engineering activities have been widely described; correspondingly the significant compression of timescales have only been possible through the pervasive application of computers to all development activities. Fig. A.2 illustrates the existing links between engineering activities and corresponding relevant computer-based tools.

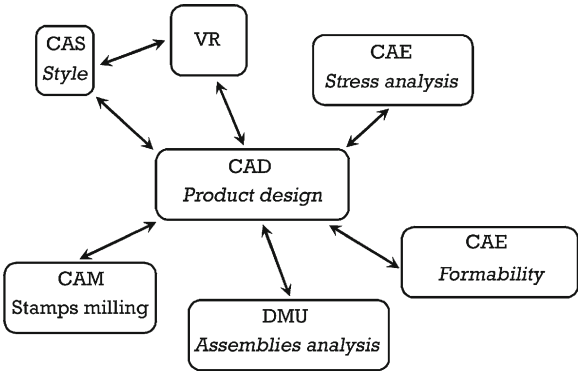

Fig. A.2 Links between product development activities and dedicated informatics tools (from Morello et al. 2011)

- Style development applies CAS tools with two different outcomes: Improving style architect productivity and generating an output (mathematical style model) that can be reused as it is by body engineers.
- Virtual reality is a computer based tool that enables representation of exterior visible surfaces with enhanced realism in context; this makes it possible to evaluate the forms and light reflections they will have in a real environment and enable their visualization from any point of view or in motion; this technique enables decision makers not familiar with drawings or information technology to be involved effectively in the decision process.
- Structural analysis is one of the major tools included in CAE that enables the evaluation, not only of the body structural integrity, but also many other aspects, from weight to drag coefficient. The body mesh, the starting point of any FE analysis, is performed by computers almost automatically, starting from CAD mathematical models.
- A particular FE analysis, performed by considering the elasto-plastic material behavior, can be applied to the design of stamps, again using CAE tools; the same body panel mathematical model, defined by product engineers, can be reused by process engineers to verify that sheets can be stamped to their shape, without risk of rips and wrinkles; similar tools are also used to assess plastic parts formability.
- CAM enables definition of the cutting tool path for milling machines that will manufacture the stamps; again the same body panel mathematical model that has been used for stamp design can be used also for stamp manufacturing.
- The computing power of modern computers enables the preparation of complete assemblies renderings with simplified surfaces, including also related production tools, applying DMU techniques, that also take advantage of virtual reality.

Such renderings offer many potential applications by:

- Style architects: Evaluating aesthetic results obtained by joining different panels taking into account gaps or profile errors.

- Product engineers: Evaluating kinematic mechanisms or interference between neighboring parts.
- Production engineers: Assessing the motion of parts along the production line while checking for collisions.
- Service engineers: Evaluating assembling and disassembling operation for repairs.

A.2 CAS, Computer Aided Styling

When the development of a new model is started, a set of general vehicle specifications is defined, essentially consisting in the following information:

- The type of car, market segment and expected production volumes,
- The relevant exterior and interior dimensions,
- The engines, gearboxes and tires to be used,
- The parts to be carried-over from previously developed models,
- The manufacturing and assembling technologies to be used in connection with the production plant selected,
- The performance and cost targets.

A preliminary layout sketch of the car can be drafted from the first five items; from this sketch, body style and structure developments are initiated. An example of a preliminary car layout sketch is shown in Fig. A.3.

Usually, each new car is born as a replacement or as a part of an existing car family; this fact generates constraints regarding the utilization of an existing platform, including car floor, chassis components and powertrain. The crucial objective is to generate a form that can excite positive emotions in future customers, which are consistent with the commercial target of the model to be developed and with the existing boundary conditions (i.e. production plant, suppliers, cost, etc.).

In this context two distinct phases in the style development can be identified:

- Form generation, and
- Mathematical model generation.

A.2.1 Form Generation

The aim of this section is to identify a number of relevant facts without trying to analyze or rationalize the creative process behind them. In developing cars, or industrial products of similar complexity, designers and engineers must closely cooperate in order to define the form of the product. The designer conveys insight through graphical elements, while the engineer brings this insight to completion, transforming these graphical elements into a technologically feasible object. To ensure continuity, it is

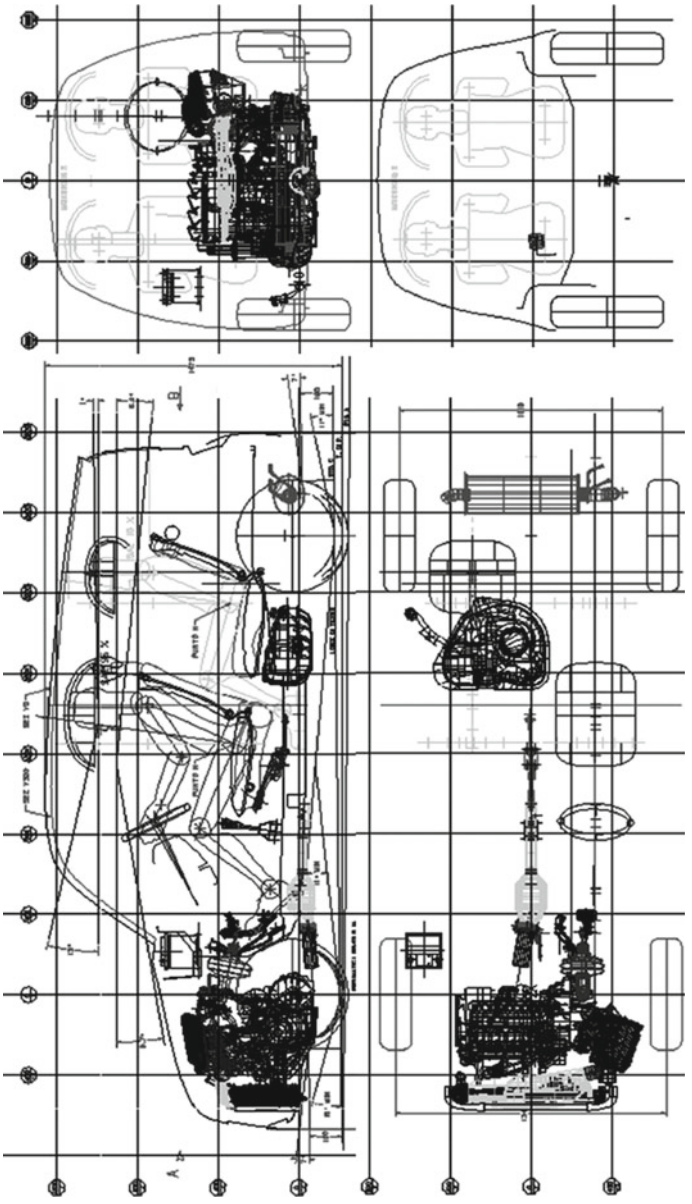

Fig. A.3 Example of preliminary car layout sketch, suitable to verify packaging, roominess and visibility; this is the starting point of body style and structure development (redrawn from Morello et al. 2011)

necessary that part of the creative background of designers is available to engineers and vice versa.

In principle there could be two different approaches to product design: develop an idea, a solution to a problem, with the assistance of scientific analyses, or alternatively use scientific analyses to define an idea. This second approach, even if desirable from a certain perspective, yields limited results and is in general only useful to solve relatively simple problems. The first approach leads usually to the best results.

Style development is a balanced mix of intuition and scientific approach, where the success of the development process requires an appropriate equilibrium between creative and structured activities. What is important is thus full understanding between two different thought processes: while it is true that the best idea without engineering development cannot become a viable product, it is also clear that the best engineering method without insight will not translate into an interesting product. During form generation, the product's appearance will summarize the designer's understanding of model targets; this understanding will materialize through partial sketches, like those shown in Fig. A.4, that only later will be integrated into a consistent form. These sketches give form to the ideas generated while capturing product targets to be integrated successively. They do not have all the characteristics required for an objective representation, but rather represent the idea as interpreted by the designer.

Still only very immediate tools such as a sheet of paper and a pencil for a freehand sketch can materialize insights and make them available for further processing. Indeed no software tool is yet available for creative activity which is quite as effective as freehand sketching, and in general few designers are able to materialize their ideas with draft and paint software tools available; only when key ideas are conceived can they be integrated into a detailed digital model. This is already a rationalization phase that seldom receives further creative contributions.

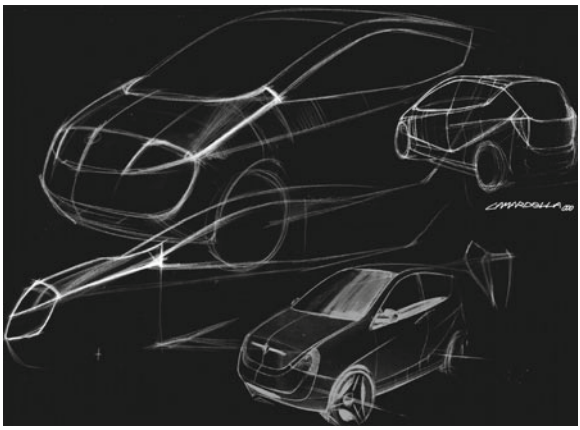

Fig. A.4 Hand drafted sketches representing the designer's perception of product objectives (from Morello et al. 2011)

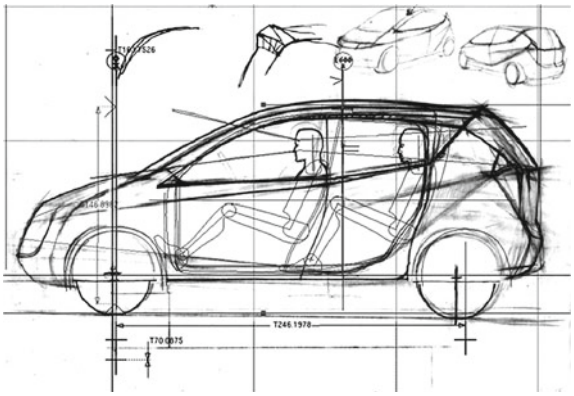

Fig. A.5 Transforming sketches into coordinate lines (on the xz and yz planes) allows obtaining a style sketch that will start discussions between designers and engineers (from L. Morello et al. 2011)

The digitalization of the initial sketches, according to the coordinate lines in the xz and yz planes, is shown in Fig. A.5. It enables the creation of a complete sketch of the car body, that can be observed from any point of view; it will initiate discussions between designers and engineers. In the past designers and engineers could discuss only using scaled clay models, available later in the style development process; nowadays rapid sketching and paint software tools enable an early interaction between these two different cultures.

A.2.2 Mathematical Model Generation

It looks unlikely, at least for the time being, that a CAD system designed to provide a complete and very detailed description of the body surface can be also used for a creation process that concentrates only on more specific aspects. Nevertheless CAD systems are useful immediately after form generation to investigate the compatibility of what has been conceived with the desired performance and the technologies involved with its production; product and process engineering require a very complete and sharp representation.

The few lines, initially defined, are now converted into spatial coordinate surfaces with the help of software tools, as shown in Fig. A.6. Missing details are added; this operation is performed almost routinely since it does not require conceiving new forms but is just a consistent development of the previous insight.

Image processing and rendering systems allow results to be verified regularly and the needed corrections to be introduced; Fig. A.7 shows one such representation. At this stage, these surfaces are used as an input for a CAD system to enable further details to be added. At this point, many shape details are added to complete

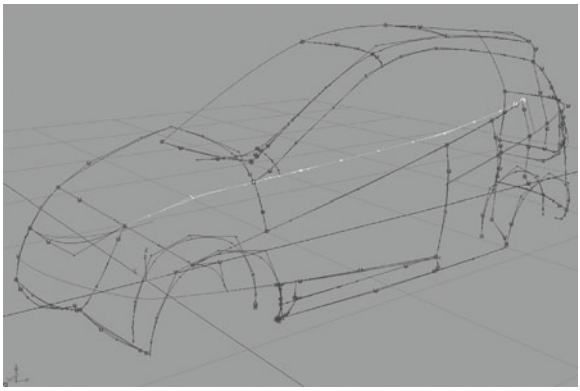

Fig. A.6 The few lines, initially defined, are digitalized and converted into spatial surfaces by means of dedicated software tools (from Morello et al. 2011)

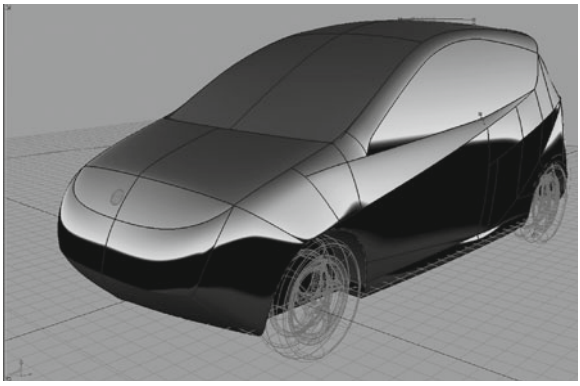

Fig. A.7 Three-dimensional rendering of initial sketches allows correction of added elements, according to their consistence with the initial insight (from Morello et al. 2011)

the surfaces; the transformation into mathematical lines of the detail of door handles is shown in Fig. A.8.

During the engineering development of the style shape many problems may arise that require a new reinterpretation or redefinition of the initial form. These problems do not regard the body taken as a whole, but more often relate to single details or the transitions between different surface elements.

A CAD mathematical model usually enables the effective evaluation of the car exterior shape, using for instance virtual reality. Nevertheless, improvements in these systems are still needed to allow each person involved in the decisions regarding the appearance of the car to be familiar with them; this is why physical models are still in use to confirm decisions taken on virtual models. Sometimes direct viewing, and the sense of touch on a full scale object, are useful to perceive the correct impression.

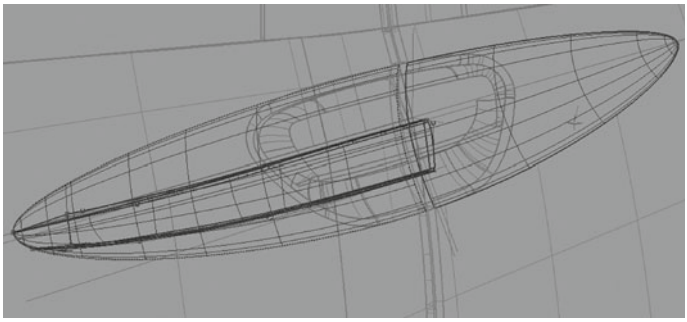

Fig. A.8 Transformation into mathematical lines of details, like door handles (from Morello et al. 2011)

Fig. A.9 Milled surface cut from a sawdust and epoxy resin block, treated with plaster and paint, to simulate the final appearance (from Morello et al. 2011)

Figure A.9 shows one of these models. They are built automatically by means of computer aided milling of a synthetic material block (a mixture of wood sawdust and epoxy resin, for instance Epowood®), starting from the CAD mathematical model directly. These milled blocks can achieve a highly realistic aspect by finishing, painting and polishing by hand.

Sometimes, corrections are introduced by designers on the model directly, to improve the appearance or to visualize and discuss possible modifications. In this case the mathematical model will be updated by digitalizing the new surface directly.

A.3 CAD, Computer Aided Design

Modern computer aided instruments enormously simplify the detailed and exhaustive representation of the surface geometry that is now represented by continuous mathematical equations; nevertheless it introduces new issues depending on the type of

CAD system in use. Those currently available on the market have comparable modeling capacity, but not identical techniques for representing surfaces mathematically; therefore the use of different CAD systems implies the use of so called universal translators such as STEP or IGES, which are two of the most common, to convert the data generated in one system so that they can be used in a different one. In certain cases dedicated translators have to be developed. Additional time must anyway be spent to convert, repair and complete the data, with consequent costs that could have been avoided by choosing a single CAD system, at least for the development of a given model.

In addition significant training time is required to use any CAD system, that, like any computer code, undergoes continuous improvements and modifications. Different systems imply different procedures to create the same geometric entities and the skills acquired by an engineer on a certain system can be applied to a different one only with some difficulty.

A decision about adopting a given CAD system is a strategic one, because of the capital investments involved for software acquisition and training, and the cost of reusing drawings developed in the past. This has an amplified effect on partners and suppliers. In spite of these inconveniences, it is relatively easy to find instances, in the recent history of car design, of major car manufacturers using different CAD systems (e.g. body engineering and powertrain engineering) at the same time.

The transfer from CAS to CAD system of these mathematical models usually does not require reworking because surfaces are simple (only the visible parts are represented) without comments, dimensions and tolerance information; the effective communication between these two systems is a major advantage of these computer tools: the same mathematical model used to represent the aesthetic surface is also used to represent part of the component and to program the milling machines cutting stamps.

Aesthetic surfaces contain not only information about their shape, but must define also their contour, including the gaps between different panels of the body skin or play between fixed parts and parts that can be opened or replaced, or between body panels and glasses. The definition of these details is a consequence of the compromise between aesthetic concepts and engineering requirements, required by part function and manufacturability.

In the next section the development of a car body is described, with particular reference to the body shell. The example described refers to a new body development, starting from an existing platform, which represents the most frequent case. In fact, the development of any major part of the platform (engine, gearbox, suspensions, etc.) requires a significant development effort; for this reason, such parts continue to be used for more than 10 years, also on very different cars.

A.3.1 Body Modelling

The most important steps of body modelling are typically the following:

- Structure architecture definition, as a function of expected production volumes, technologies and materials;
- Definition of the main sections of the skeleton, partly independent of the style model;
- First approximation modelling of body exterior panels;
- Detailed analysis of junctions between side members, cross members and pillars;
- Trade-off between aesthetic, structural and manufacturing requirements.

Structure architecture

The first step is the definition of technological and design solutions that will be used for the body under development. To shorten development time, including modelling, virtual and physical validation, solutions are preferred that have already been applied on other cars or validated in previous non-finalized development activities (so-called pre-engineering): these solutions are usually conceived as *archetypes*, meaning a generalized model, useful for subsequent application to an assigned exterior style or shape .

Archetypes are not only the consequence of a structure architecture, but also of the assembling process or materials selected. For instance, on a large production car, the most common body archetype is the unitized one made of stamped steel, while for a small production volume a partly not unitized solution could prove more convenient.

The term archetype is all-embracing because it includes many different design aspects such as, for instance, the impact of aluminium use, with the possibility of using extruded or cast parts, or laser welding, with the elimination of welding flanges and electrodes passage holes.

Main sections

According to the selected archetype, including the structure architecture, material, applicable forming and assembling technologies, characteristic cross sections of the skeleton are defined (see, for example, Fig. A.10).

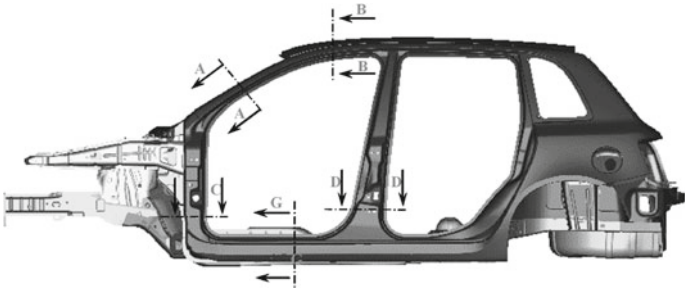

Fig. A.10 Some typical body cross sections that can be defined starting from an archetype (from Morello et al. 2011)

Starting from an archetype, even if not yet applied to an assigned aesthetic surface, many functional parameters are conditioned such as:

- The dimensions of resistant cross sections,
- The thickness and material for each of its parts,
- The aesthetic matching with neighboring parts, for instance parts that can be opened or made of glass,
- The assembling solutions for small components such as weather strips, hinges, locks, etc.

To understand how all this information can be focused in a few lines in practice, reference can be made to Fig. A.11, where alternative configurations for section B–B of Fig. A.10 are shown, corresponding to the part of the roof above the front door.

Four different archetypes can be observed:

- Archetype 1, characterized by a longitudinal aesthetic strip covering the welded joint between the roof and the body side, by a sliding glass without visible outside frame and by a weather strip integrated with the guide liner of the glass.
- Archetype 2, characterized by an enveloping roof with no covering strip, framed glasses and weather strip mounted on the welding flange between the roof and the body side.
- Archetype 3, again characterized by a longitudinal cover strip, integrating also the function of weather strip.
- Archetype 4, similar to archetype 2, but with frameless glasses and integrated weather strips and glass guide liner.

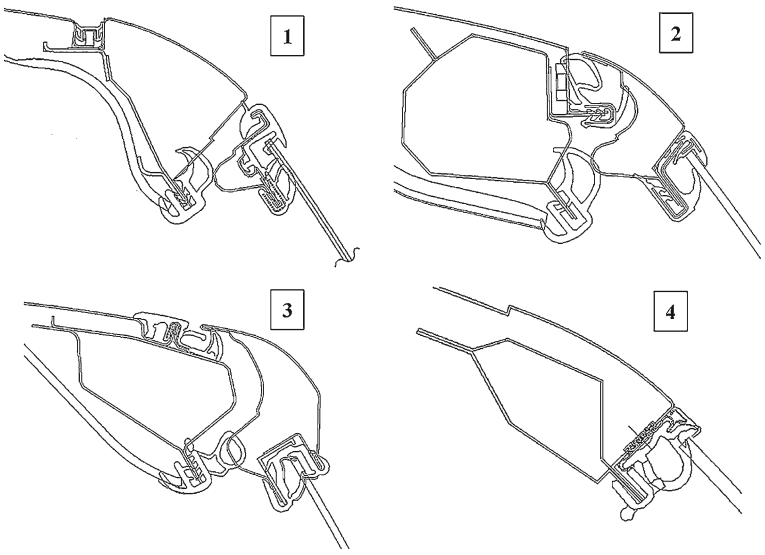

Fig. A.11 Some different archetypes for joining the roof with body sides, depending on the door archetypes that can be matched (from Morello et al. 2011)

Different archetypes have different aesthetic contents, also corresponding to different capital investments, and procurement and production costs, as a function of the different structure architecture and materials. It is important to remember that these sections can be applied to the specific body only if they are adapted to the mission to be accomplished and to the specific shape of the car style.

This archetype selection and adaptation process can be performed not only for major components, but also for details such as weather strips and glasses. To speed-up this process and avoid mistakes, it is important to access a wide database of already developed in-house or competitors' solutions.

This operation consists of repositioning on the new style and resizing already existing elements, corresponding to production cars or pre-engineering results; other components may be used as-is, i.e. without adaptation, e.g. the weather strip section, locks, hinges, etc. This geometry will be subsequently refined following analysis and virtual or physical prototype testing.

Modelling

Once a number of sections have been positioned and sized in sufficient quantity to define the body shell critical areas, engineers proceed modelling the remaining body shell parts, doors, hood, etc. Critical areas usually include the structural skeleton and the doors hinges.

To clarify this process, a body shell conceived as a space frame may be considered, as in the example of Figs. A.12 and A.13, since it is easier to identify beams and junctions on the body side. For instance, in section B–B (Figs. A.11 and Fig. A.10), the archetype that better matches the example is 1. Based upon this cross section (and clearly a number of others along the door contour) the upper part of the body side and its upper beam can be modelled in detail. Existing CAD systems enable this operation to be performed almost automatically, thanks to their parametric and associative features.

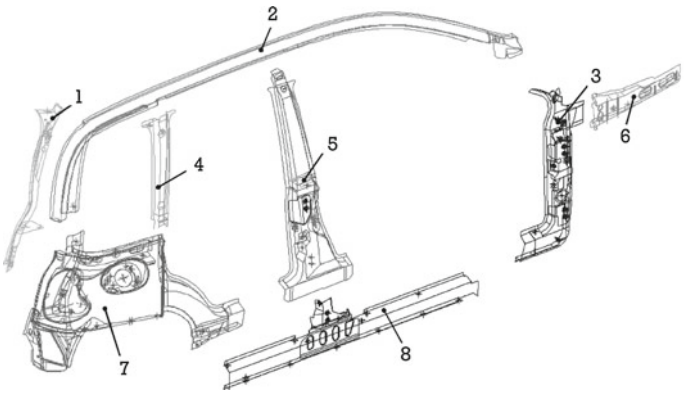

Fig. A.12 Basic components of the body side of a space frame type body (from Morello et al. 2011)

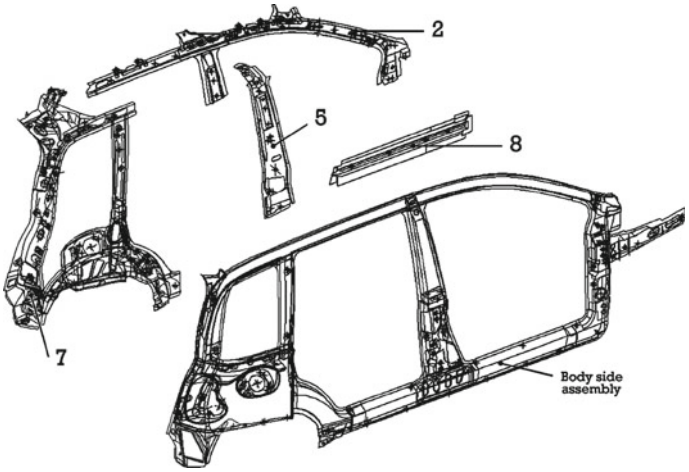

Fig. A.13 Body side assembly of the previous space frame body (from Morello et al. 2011)

The upper beam to be modelled is logically connected to the aesthetic surface (it is associated with the surface) and its size is defined by the measurements as a function of a limited number of fundamental dimensions (parameters). These parametric and associative features also allow implementation of the many modifications to be expected in a short time; for instance, CAD systems with these features allow an entire model to be regenerated, as a consequence of a style modification, maintaining the archetype logical relationships automatically.

The power of the associative features can be exploited to investigate the effect of a modification also to other geometric entities, such as stamps, milling paths, finite elements analysis models, etc. This kind of approach can be repeated for all body elements whose geometry can be assimilated to a cross section extruded along a curved path.

Stamped steel or aluminium body panels may be represented as a portion of solid space included between the aesthetic surface and a similar surface obtained by shifting the previous one by the panel thickness. A line obtained on a drawing by cutting the aesthetic surface is called *style profile*; the other line defining the panel section is obtained with a pure shift. This process may be applied with some caution to thicker elements, such as plastic components. Further elements, such as ribs, roundings, pins, etc. may also be defined using archetypes.

Some car manufacturers, on the contrary, opted to model also surface-like parts with solid bodies, thanks to CAD systems designed for this feature: this procedure involves greater modelling time, but enhances the subsequent development steps, such as designing stamps for high thickness plastic components.

Junctions modelling

When structural beam elements of the body are modelled, the junctions at beam intersections can be defined in detail. To designate these junctions, a standard nomen-

clature has been defined using letters: it is interesting to note that the order adopted puts in the foreground the areas more bound to style than to structural behavior. Consider, for instance, junction A, at the intersection of body side with windshield and roof: The components of the body shell involved (see Fig. A.14) are the roof, upper windshield cross member, exterior body side, front or A pillar cross section and reinforcement member. At this joint also the windshield and its structural adhesive bond contribute, and the geometry of any liner may be involved. The front door and their weather strips are also affected by this geometry, as is the space available for driver and passenger and their visibility.

Together with the space requirements for the installation of these elements, the structural requirements relevant to torsional stiffness, front impact, roll-over should also be considered; the assembly cycle feasibility should also be considered. If classical spot welding is chosen, also access for the electrodes should be taken into account. For example (see Fig. A.14 , at right), the eyelet surrounded by a dotted line allows access to the electrode of the welding tool from the inside of the body and therefore makes the junction between roof and body side possible.

Also the task of designing different junctions in detail is simplified by CAD systems, enabling 3 D modelling, with a clearer perception of geometrical issues, together with quicker modification or adaptation of existing pre-validated solutions, therefore shortening the development time.

Test validation

Once the body has been defined, including doors, hood, hatch and removable parts, together with all detail interfacing body components (such as weather strips, locks, hinges, etc.), a complete 3 D model is available that can be easily tested with respect to different perspectives. Each virtual test will result in modifications for surfaces or sections; with a parametric associative CAD system, each will be implemented in a very short time, sometimes automatically, and transferred also to associated entities such as stamps, assembly fixtures or other dedicated production tools.

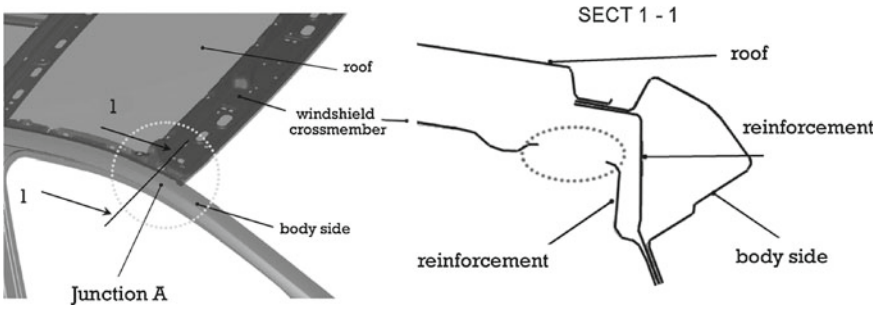

Fig. A.14 Junction A modelling, at the intersection of body side with windshield and roof (redrawn from Morello et al. 2011)

CAD system speed is particularly expedient when introducing a large number of modifications resulting from potential malfunctions detected during the virtual validation tests.

As far as aesthetics is concerned, mathematical models obtained with this procedure enable the refinement of the exterior surfaces with style architects and certify consistency between shape, performance and manufacturability: for instance, the shape required for the windshield by the style concept is verified in terms of visibility and installation of wipers, or for side glasses again in terms of visibility and sliding motion into the door.

The body mathematical model can be transferred for evaluation in terms of structure analysis, regarding dimensions, local thickness, material choice and welded junctions. Also in this case, computer tools contribute to shorten development times by generating the calculation mesh almost automatically. In this way, the mathematical models become an effective communication tool among engineers, stress analysts and, again, style architects, to negotiate modifications and define trade-offs. A similar situation enables process engineers to evaluate and analyze the stamping and assembling process.

The mathematical model is built in the ideal hypothesis of nominal dimensions, without taking into account the effect of fabrication tolerances. However, using dedicated software tools, mathematical modelling enables investigating the effect of dimension variations on the assembling process and compatibility with product performance.

A.3.2 Rules and Common-Practice in CAD Modelling

CAD models are the transposition into mathematical parameters of a set of numbers that regard not only the geometric nature of a part, but also its technical and organizational features. The information regarding geometry includes the coordinates of points, surface and lines equations, etc., needed to define the shape of a part completely. Part of this geometric information has also some organizational content; for example, the associative features describe, in computer language, the operations accomplished by the design engineer while modelling a part (design intent) and their relationship with neighboring models (welding and assembling interfaces); this information allows the regeneration of the mathematical model automatically when some of its geometrical parameter are modified.

Technical features cannot directly infer geometric information, containing for example dimensional tolerances, positioning reference points, functional specifications, etc. that are needed for part operation, manufacturing, or production fixtures. Nominal dimensions are instead usually inferred from the mathematical model.

Organizational features consist in data needed to manage the part within the company information system according to usual company practice. Among the organizational information, the description of the product configuration is the most relevant; product configuration describes the logical relationship between any of the parts of

the vehicle. Product configuration enables the correct identification of any subassembly or elementary part and the preparation of a bill of materials.

Product configuration description allows also the creation of any assembly drawing and the management of material flow along the production line, orders to suppliers and the delivery and storage of spare parts.

A further organizational feature to be recorded on mathematical models is a note concerning their development status; it is needed to inform any of the potential users of a mathematical model about the level of risk of processing information that has not been fully validated since many activities are performed in parallel by people with real-time access to a common data base.

Finally, CAD models are classified with reference to their content and to their preparation technique. The following classification is usually applied with regard to the content:

- Outline drawings, essentially useful to the design engineer to develop ideas, define critical matching between parts and solve problems of geometric compatibility.
- Assembly drawings, useful for documenting how parts are assembled together.
- Part drawings, useful for exhaustive documentation of dimensions, materials, specifications of a single part.

The following classification refers, instead, to preparation technique influencing the kind of model used, the main ones being:

- Wire frame models, i.e. 3 D models where solid bodies are represented by spatial curves describing their edges; between one curve and the next, the surface shape is unknown and must be interpolated.
- Surface models, i.e. 3 D models where a part is described through its contour surfaces; the coordinates of each points are fully determined.
- Solid models, i.e. 3 D models including a complete description of the space included between the boundaries of the model and representing every detail of a part, including its physical properties such as mass, moments of inertia, etc.
- Conventional drawings. They are paper print-outs, similar to a pencil drawing, used for communication only and unsuitable for further development.

Reference frame

The reference frame traditionally used by body engineers is different from that suggested by the SAE J670 standard for vehicle dynamics mathematical models; here an xyz axis system is defined, with its origin in the body symmetry plane, at the intersection with the front wheels axis of rotation and with the axes defined as follows:

- the x axis is contained in the symmetry plane and set horizontally, pointing rearwards,
- the y axis is perpendicular to the symmetry plane, pointing to the right with respect to the driving direction,
- the z axis is consequently vertical, pointing upwards.

If the vehicle body were not symmetric, the xz plane would be assumed to be coincident with the vertical plane.

The definition of the origin depends upon the position of the suspension, which determines the centre of the front wheels and the body pitch angle; therefore, this definition must be applied assuming a reference load condition, usually corresponding to a full tank of fuel and four passengers of 70 kg of mass each, with 40 kg of luggage in the trunk for cars with four or five seats, or two passengers and their luggage in two-seater cars. For different kinds of vehicles (vans, minibuses, trucks, etc.) a load condition close to full load is usually selected.

Considering the body size, and the fact that drawings should be printed at least at full scale, a complete body assembly is seldom represented on the same drawing for sake of clarity.

To enable the correct location of partial assembly drawings or part drawings, a quoted grid is represented on each drawing, according to the local applicable coordinates.

Surface representation

Body part drawings usually contain surface elements that are fully defined by a mathematical model; large surfaces are represented by joining a sufficient number of patches, whose size depends on the local curvature: a higher curvature requires a larger number of small patches.

Visible parts of the body surface are called aesthetic surfaces and are coincident with the style model.[1] In the case that the aesthetic surface is not available as a mathematical model (this was commonplace until just a few years ago), style architects must provide a physical full scale 3 D support representing this surface; this support will be digitalized point by point, for example at the intersections of the surface with the body reference reticule; the lines obtained are joined with interpolated mathematical patches as in the other case.

Each section of the drawing representing a part contoured by the aesthetic surface will contain also the style profile, the intersection of the aesthetic surface with the section surface. The concept of style profile applies also to solid models, for instance high thickness plastic parts.

Skeleton surfaces do not usually contain parts of the aesthetic surface; nevertheless they are represented with the same system, developing a surface mathematical model for the side of the skeleton matching with visible parts, taking care to define a single style profile for each of its parts. Where the aesthetic surface is interrupted, for example at a door contour or near a removable part, the mathematical surface will be cut by a surface determined by an envelope of constant diameter circles with their centre on the aesthetic surface; this operation enables a constant gap between different parts to be generated.

[1] The following indications are not standardized but refer to the praxis of a large car manufacturer and his suppliers. There are no internationally applicable standard rules for the time being, even if similar rules are widespread.

Subsequently the two parts of the surface are rounded to reproduce the effective shape of the part that can be obtained by stamping or bending. Flat surfaces might be added, to join the outside body panel to the skeleton. These are called completion surfaces, for comparison with the aesthetic surface.

Drawing surfaces are usually classified in classes (A, B and C class) with reference to the accuracy of their mathematical model. The accuracy is measured by comparing the mathematical surface with the aesthetic surface and measuring the continuity between patches. Classes are useful to speed-up the activity of style architects and body engineers, improving time and manpower efficiency with regard to applying the finishing touches when the style freeze event is still far away and many major modifications could still be needed.

Class type represents, therefore, not only the accuracy of the mathematical model, but also the maturity of the project: from class C, used for feasibility studies and the first style proposals, drawings are refined up until class A, at the end of the project, to represent the part to be put in production.

Common practice is that:

- At the initial stage, when more alternative style proposals are under evaluation, class C is allowed in each mathematical model;
- when a style alternative is selected, but uncertainties and variants are still present, class B is allowed;
- final drawings, ready for production, must contain class A surfaces only.

Specifications for each class are the following:

- Position continuity. The distance between each point of the edges of two neighboring patches must be no more than 0.01 mm, for Class A; no more than 0.02 mm, for Class B and no more than 0.05 mm, for Class C.
- Tangents continuity. The angle between the tangents to the surface on the edges of two neighboring patches must be no more than 0.1° , for Class A; no more than 0.2°, for Class B and no more than 0.5° , for Class C.
- Shape tolerance. The shape tolerances are measured by comparison of a surface patch with the counterpart on the aesthetic surface. they must be class no more than ±0.5 mm, for Class A, no more than ±1.0 mm, for Class B, while for Class C surfaces shape tolerance is not applied.

However class A surfaces could show other unacceptable aesthetic defects; to correct these before stamps milling and finishing, aesthetic surfaces are represented by means of special rendering systems, sometimes available in CAD systems, suitable to represent light reflection on the actual painted body surface.

The simulated lighting system is, traditionally, a linear source lamp (neon tube lighting) that can highlight each of the defects to be corrected; Fig. A.15 allows the difference between inaccurate surfaces or class A, well refined, surfaces to be perceived.

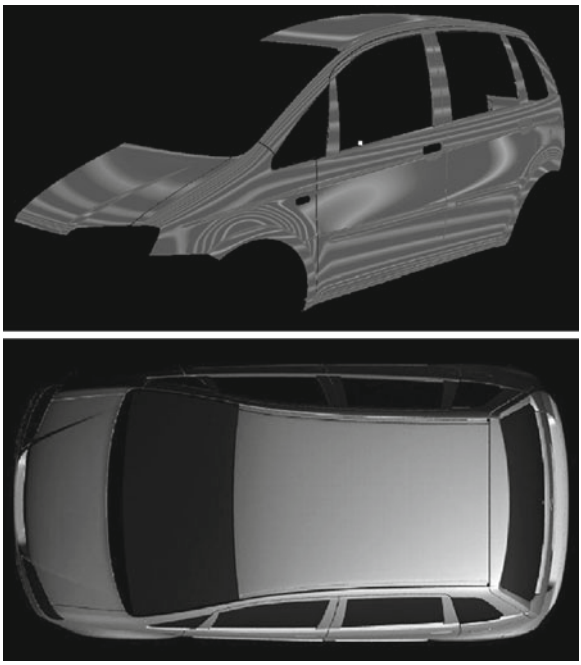

Fig. A.15 Light reflection representation for a complete body with good (*below*) and poor (*above*) quality surfaces (from Morello et al. 2011)

A.4 DMU, Digital Mock-Up

A major portion of the development costs of a new car corresponds to prototype building and testing; newest development projects take advantage of DMU to lighten part of this burden with the so-called virtual prototypes and virtual tests, providing an enormous advantage through the increasingly detailed graphical representation of real parts.

An example of two complete under-hood environments is shown in Fig. A.16. The high graphical complexity makes this kind of representation not viable using a traditional CAD system. A DMU system enables the assembly, in a suitable application environment, of all parts that should be examined; these parts must be available as independent CAD mathematical models.

A DMU system allows studying the interaction between each component with the assembly, in order to search for potential interference in their final position or during assembly, disassembly or motion according to their function. It is therefore a virtual representation of objects supporting the development process of both product and production tools.

Virtual reality, although based on a different technology, can be considered to be an implementation of DMU featuring a higher representation realism. DMU takes

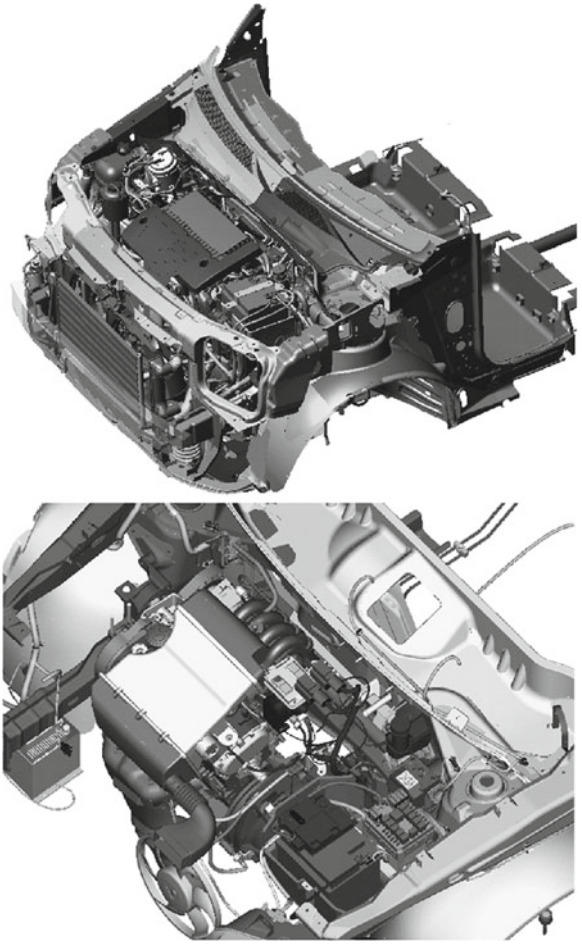

Fig. A.16 Two examples of a DMU of the complete under-hood environment; the high graphical complexity makes this representation not viable with a traditional CAD system (from Morello et al. 2011)

advantage of visualization systems that are able to manage very large assemblies, such as an entire car body, with interior trimming, an engine compartment or a platform, complete with all mechanical components. These systems approximate the boundary surface of each component with simpler elements, e.g. triangles, obtaining a simplification in terms of the information describing the objects to be represented. This technique is called tessellation or tiling.

To provide a general picture, the file representing the assembly can be reduced by ten times in size. This reduction is usually performed off-line with suitable translators, interfacing original CAD models with the visualization system; the representation error introduced by this operation can be controlled by the user.

Fig. A.17 DMU of a complete body shell. This figure reproduces what displayed by a computer monitor, showing the product breakdown structure on the left, with the names and part numbers of each component or subassembly included in the model (from Morello et al. 2011).

An important further advantage provided by the DMU system is the possibility to manage, in the same representation environment, mathematical models from different CAD systems; their diversity, justified by previous choices or by particular design aspects, is overridden when the models are to be translated in any case to a different common format.

In addition, the reduction in mathematical complexity of these models makes them usable on personal computers; these models are thus available also to people not directly involved in the design process, making a wider sharing of information possible.

The virtual prototype (the entire vehicle or a large part of it) represented by a DMU system can offer each working group a single and reliable reference, offering the advantage of managing each component in its real environment. Finally DMU systems are able of storing the product breakdown structure, identifying each part included in a given assembly. A last important implication of DMU is that working in different locations or different companies is facilitated by a common assembly model of reasonable size than can also be shared through the internet.

An example of a complete body shell DMU is shown in Fig. A.17. It shows what is displayed by the computer monitor; on the left the work breakdown structure shows part number and name of each component or subassembly in the assembly.

The product breakdown structure is usually imported from the company information system before initiating the implementation of the digital mock-up, helping to build up a complete assembly from its parts without omitting any. The same structure is used as a navigation tool to reach easily each of the parts in the assembly or to build and check partial subassemblies, available along the production line, before completion.

The digital mock-up not only simulates the final shapes of the body but stores its parts in hierarchical systems able to simulate the body assembly process, in the same sequence as developed along the production line. The first application of the digital mock-up is composing assemblies, to look for errors in their components, since the high complexity of components geometry makes shape errors quite likely.

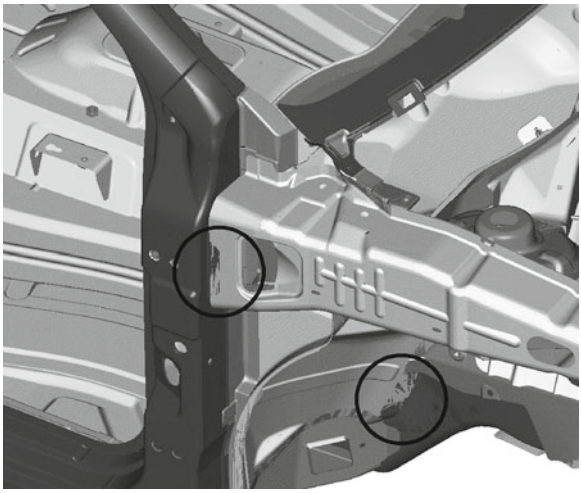

Fig. A.18 The *circled areas* in this picture show color changes that indicate interpenetrations of contacting parts due to modeling errors (redrawn from Morello et al. 2011)

Assemblies visualizations are usually made by assigning to each component a different color that is altered when the relevant part is selected (although the grey tones prints of this book are unable to illustrate this). By examining Fig. A.18 it can be realized how flanges or spot welds disappear when assembling a large number of components in a single assembly and an interpenetration between different elements can be discovered. This occurrence is more likely during the initial phase of the mathematical model development of body panels or when assembling a trimming element on the body for the first time.

To correct these errors, the following checks can be performed directly within the digital mock-up environment:

- Geometry compatibility between visible elements of different parts.
- Building local cross sections and measurements of distance between parts not immediately visible. This operation can be made quickly, even on two remote personal computers connected on line, for example during a teleconference.
- Potential interference during assembly.
- Geometry compatibility in dynamic conditions, when some element is deformed by external forces.
- Feasibility of kinematic displacements.

Figure A.19 shows how it is possible to represent the complete body shell with a multi color shadowed model in the digital mock-up environment and to open, in the meantime, a window where a cross section along an assigned plane is quickly made. This plane can be translated in any direction to investigate the entire interface between two parts. This procedure allows one to easily study a new assembly, as it may occur when an assembly is developed by a supplier or is carried-over from an

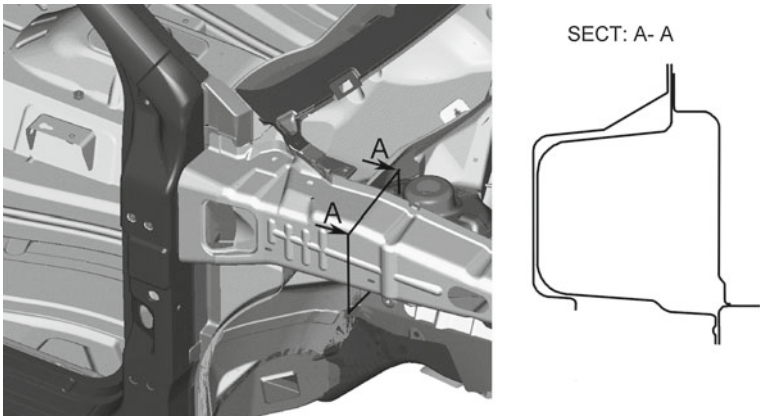

Fig. A.19 Automatic creation of a cross section to check for body interpenetration (redrawn from Morello et al. 2011)

existing model. Apart from instant sectioning, the temporary elimination of some part is also possible, to concentrate the attention on single elements of the assembly.

By looking at the enlargement at the right in Fig. A.19, the lines correspond to the style surface of different parts. When actual parts are in contact, section lines of the style surface are separated by the sheet thickness. This feature must be kept in mind to avoid misinterpretations while checking models for gaps and interpenetrations. Measurements can be taken also on cross sections (see Fig. A.20): This function enables a quick check of part dimensions or gaps in the welding flanges areas. As mentioned previously, these operations can be performed by people not totally familiar with CAD modeling.

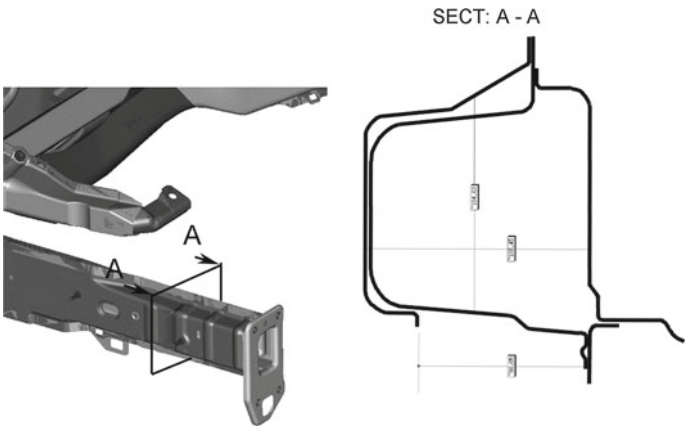

Fig. A.20 In the digital mock-up environment, dimension measurement is easily made, to check for part geometry or gaps (redrawn from Morello et al. 2011)

The only virtual tests not performed with digital mock-up systems are those related to dynamic and structural performance, that are investigated by different simulation models. the main examples of digital mock-up applications are:

- Drawings check,
- kinematic analysis, and
- Evaluation of assembling and disassembling feasibility.

A.4.1 Drawings Check

Drawings are checked to verify their accuracy and compliance with company's design rules. Digital mock-up assemblies are examined according to dedicated check-lists that enumerate rules to be observed and certify the compliance of related drawings. The person in charge of this check is not always the person in charge of the drawing and its related modification, and could also be an internal customer of this drawing. These check-lists become thus a tool to enhance a structured discussion between members of the different working groups.

Check-lists of an assigned assembly could consist in, for example, a table reporting, in the rows, the functions to be performed and, in the columns, the components of the assembly involved in these functions. Each of the verifications to be made should refer to a written rule documenting this function objectively. At each intersection between rows and columns the table should report 'yes', 'no' or 'not applicable' with respect to the question of compliance with relevant design rules.

If during prototype testing a malfunction is detected in an area covered by an item in a check-list, some decision must be taken by all those involved in the design process of the related component or subassembly. Not only must this error be corrected, but the rules that allowed this error to occur must be modified as well. Thus company rules are modified to avoid this error occurring again in the future or new control items are added to the check list.

A typical list of functions to be verified in a part or subassembly of the body should include the following categories of checks:

- Drawing completeness (dimensions, tolerances, surface finishing, etc.).
- Visibility of stamp split lines (which should never be visible from viewpoints corresponding to the normal positions of driver or passengers or should be concealed by dedicated trimming).
- Assembling and disassembling (these conditions are not equivalent, because assembly shop cycles cannot be reproduced in service shops; for obvious reasons, in principle, each part should be replaced without requiring disassembly of other parts).
- Interference between parts or contacts (if not correctly treated, contact points are a potential source of squeaks and rattles).
- Utilization of parts with dimensions at the limits of the allowed tolerance field.

- Dust and water tightness of passenger compartment and trunk (treatment of junctions between parts separating trunk and passenger compartment from the outside).
- Separation between electric harness or hot parts and flammable materials (prevention of fires after vehicle crash).
- Separation between power and signal electric harness (prevention of malfunctions due to electromagnetic interference).

As we have seen, the digital mock-up easily allows the measurement of distances between parts; this can be done by drawing cross sections in the critical areas of the assembly. This procedure looks to be insufficiently productive when verifying large body assemblies, such as the engine compartment, the underbody or the very congested space between dashboard an firewall. Figure A.16, illustrating two assemblies of engine compartments, highlights the difficulty in identifying all potential interferences or dangerous proximity points between parts to be checked. In addition, such verifications should be performed not only in static conditions, but also in any position a component may take during vehicle operation, considering for instance the powertrain motion on its suspension due to road bumps and torque variation.

All digital mock-up systems offer the possibility of automatically looking for points of neighboring parts closer than an assigned set point and sorting out components in the assembly according to their function in the product breakdown structure.

Movable parts (for instance wheels, during their steering motion) can be introduced in the assembly as an envelope body encompassing all potential positions during vehicle operation.

A.4.2 Kinematic Analysis

Kinematic analysis finds important applications in body engineering while designing mechanisms of moving parts, such as doors, hood, trunk lid and other mechanisms as wipers, sliding glasses, locks, outside mirrors, etc. The objectives of this analysis are:

- Validation of the working of the mechanism,
- interference of moving parts that become closer during their motion,
- positions of stops limiting the mechanism motion, and
- evaluation of speeds, accelerations and forces during mechanism operation.

Consider, for example, Fig. A.21 showing the extendable hinge of a lateral sliding rear door of a minivan: The digital mock-up of this subassembly includes the mechanism itself (the extendable hinge), the fixed related components, such as the body side, the sliding rail and the front door, and the movable part, such as the sliding door and its interior covering panel.

One highly useful feature of a digital mock-up is that each part in the assembly is loaded into the model from the company data base at its present status of development; once the model is set up, it is possible to repeat any verification as soon as a new

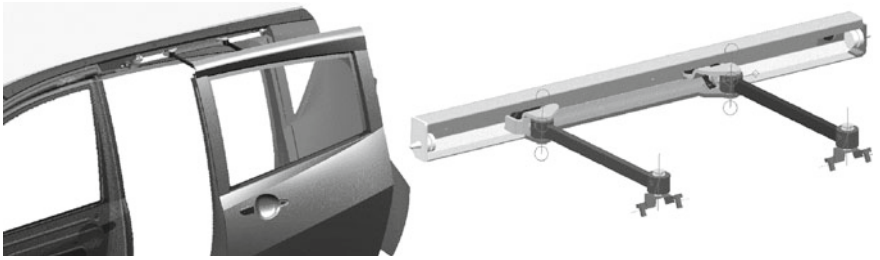

Fig. A.21 Digital mock-up of an extendable hinge of a sliding door (from Morello et al. 2011)

element in any of its parts is added or a modification introduced. If new modifications are needed to allow the operation of mechanisms, they can be introduced in the same working section and checked consequently.

The mechanism is represented by defining the following elements:

- Kinematic couplings between mechanism parts, such as cylindrical, spherical or sliding bearings,
- external shape of moving and fixed parts, and
- extension of the rotary or sliding stroke of the elements of the mechanism.

The digital mock-up allows only kinematic motion without friction and can only verify geometric compliance; nevertheless it can be used to calculate the input functions for a multibody model of the system dynamics, suitable for providing a full evaluation of system performance, including dynamic forces.

A.4.3 Assembling and Disassembling Evaluations

A further design requirement of complex systems (such as the car body) is the compliance of shapes and dimensions of each component with an existing assembling shop and cycle; this compliance is not only related to parts dimensions, but also to the compatibility of these parts with the welding, assembling and transportation fixtures of the production lines. This problem has already been mentioned when referring to check-lists; this section deals with the digital mock-up functions involved in this verification.

Considering, for example, the front part of the engine compartment lower rail: The complete assembly obtained as a result of a number of operations defined by the assembling cycle is shown in Fig. A.22. In the same figure an exploded view of the parts involved in the assembling is also represented: Without entering into the details involved in this set of operations, it is possible to imagine identifying, through a number of trials, possible operations sequences achieving the required result. If different sequences obtain the same result, the most expedient should be selected by taking into account:

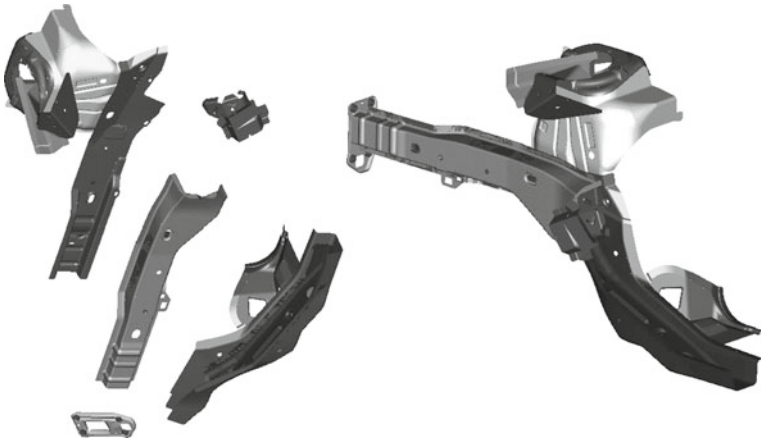

Fig. A.22 Automatic design of a subassembly made by a digital mock-up system, starting from the CAD mathematical model of each part (from Morello et al. 2011)

- The number of loading and unloading operations of parts on the welding and assembling fixture,
- the final dimensional tolerance that can be obtained, and
- the possible deformations on the assembly due to thermal expansion caused by the spot welding sequence.

The digital mock-up proves to be a very useful tool to initiate working team discussions or topical verifications. Many significant mistakes can be avoided during a free preliminary multidisciplinary discussion. The examples introduced should enable the usefulness of the digital mock-up in its main applications to be appreciated.

These virtual analyses become increasingly accurate as the digital tools improve; nevertheless actual tests on physical prototypes must be performed, at least for final product validation; their cost is however lower due to the increasing number of errors corrected at the virtual stage.

A.4.4 Virtual Reality

This final section highlights the role of Virtual Reality (VR) in enhancing engineering design, describing this tool in conjunction with digital mock-up since, in fact, virtual reality may be thought as the most sophisticated tool to represent and navigate a large detailed assembly. This technique allows one or more user to interact simultaneously in a simulation environment controlled by computers; this simulation can achieve greater realism than that available while interacting with a model by using a conventional monitor and a mouse, making operations more intuitive, effective and quick.

Due to the fact that these systems are still evolving, some information regarding the hardware is also included, while realizing that new developments will make virtual reality simpler, less expensive and, therefore, more widely applied. Many interface devices exist that provide the illusion of seeing, touching and manipulating virtual objects; their common characteristic is granting people, working with this simulation, the possibility of viewing from any direction, providing high levels of visual perception and sense of involvement; visual feeling can be enhanced by hearing and touch.

Virtual reality is a technology that can be used to enhance natural human capabilities or exploit those usual capabilities that appear only in front of a physical prototype of the object under examination. The ultimate target is, again, to reduce development time and costs, bearing in mind that traditional interfaces such as keyboard, mouse and monitor effectively force engineers to work within a limited and unnatural bi-dimensional space, requiring a high capacity for abstraction and imagination which not everyone has.

An ideal virtual reality system should possess at least the following features:

- High resolution stereoscopic visualization; human eyes can distinguish punctiform objects seen under an angle of $1'$ (i.e. two dots with mutual distance of 0.58 mm, at 2 m from the eyes), and give a full representation of any object in the semi-space containing the optical axis, and
- update of objects in motion with respect to the point of view, in a time lower than 10 ms and with a time lag of less than 20 ms. When images are obtained by using multiple projectors, outputs synchronization must be perfect.

In addition, systems possessing also non-optical outputs should provide:

- Full stereo sound output of both environment and object noise, with a frequency response in the range $16 \div 25{,}000$ Hz, dynamic range of at least 90 dB and background noise lower than 30 dB, and
- tactile and force feed-back, as functions of object displacement suitable for human motion capability.

The first virtual reality experiments were performed with flight simulators, developed by the Massachusetts Institute of Technology in the 1960s; a crucial contribution to this technology came in the 1980s from Silicon Graphics, a company leading the production of powerful and relatively inexpensive computers. The first applications mostly addressed the training of aircraft pilots. Virtual reality was thus developed to better visualize objects simulated by computers. Further developments followed, allowing to simulate the physical properties of a vehicle to verify different functions, such as internal and external visibility, access to the passenger compartment, space availability while interacting with the vehicle, etc. In the case of style development, a more complete representation of an object, in motion or seen by a moving observer, can be obtained.

Figure A.23 can offer an idea of the performance currently available for representing the outside of a car, starting from a CAD surface mathematical model,

Fig. A.23 Virtual reality model of the exterior shape of a car obtained by CAD surface mathematical models (from Morello et al. 2011)

in spite of the relatively poor quality of the black and white picture and the fact that the results of VR cannot be represented on paper.

Not only a high resolution representation, but also the interaction with the model are required, allowing the operator to manipulate the objects in the virtual environment. The interaction of the user with the model is possible with a full-immersive environment or by improvements of the current practice. A simulation environment is considered to be full-immersive if the operator is completely insulated from the real world, independently of the technology applied to the simulation.

An immersive simulation can be, on the other hand, more or less intrusive depending on the extent the simulation tools available to the user feel natural. For example, a 3 D visualization helmet could be immersive and intrusive at the same time. Another issue is the so-called presence level of the user in the virtual environment. The presence level is high if the user can also see his body during his experience in the virtual environment; on the contrary it is low if his body and those of other operators can only be shown by virtual representation.

The features of an immersive simulation include the following:

- The virtual environment can be observed in a natural way, offering realistic views when the head is rotated;
- The view is stereoscopic and allows perception of distances between virtual objects;
- Virtual objects are perceived in their natural size;
- There are devices addressed to the manipulation and control of virtual objects.

The illusion of living in the virtual environment may be enhanced by sound.

Virtual environment

The virtual environment usually consists of a realistic representation of virtual objects (a vehicle and its components) in a related outside scenario (i.e. show room, production shop, repair shop, etc.). Geometrical accuracy is very important, as is

the accurate definition of colors, textures, light spots and their correct reflection on surfaces, according to their gloss.

Texture is, in this case, the repetition of an ornamental drawing on a surface, that can be deformed, e.g. representing a decorated fabric upholstery covering seat stuffing or the grain of a dashboard surface, simulating leather. This can be better explained by Fig. A.24: The simulation system is supplied with an elementary drawing of the cloth decorative pattern. The simulation software repeats this drawing indefinitely, covering an assigned surface (in this case, the interior side panel of the door), taking into account the deformation of the cloth on stuffing, that is simulated by a full deformable, non-extendable surface.

Virtual objects can be created by a dedicated 3 D modeling tool or can be imported from an existing CAS or CAD model. In any case, the description of these models not only includes the mathematical equations describing their surface, but also information about the aesthetic nature of their visible surface (influencing how light is reflected or diffused) and, sometimes, about forces (mass forces, resistance, elasticity) related to their displacement.

The virtual environment controls object motion with procedures considering dynamic rendering and dynamic simulation; while parts are displaced, potential collisions are controlled by dedicated software.

The environment status is influenced by inputs that are usually the positions of head and hands of operators, while outputs are video, audio and feed-back force. Some dynamic objects can be defined without any space constriction, while others are physically constrained to move within a set of boundary surfaces. For instance an observer's head evaluating the external visibility of the car, from the driver's seat, is constrained to stay within the passenger compartments. When the head is moving

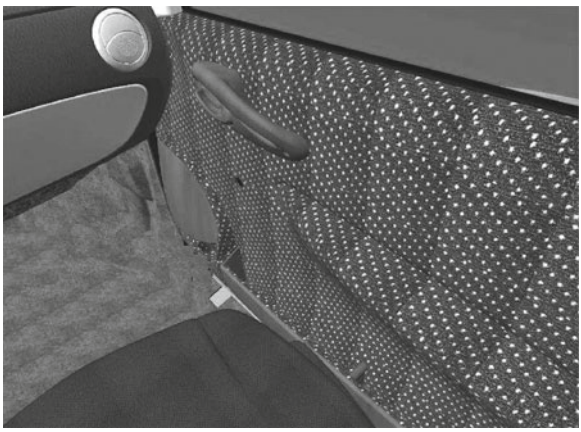

Fig. A.24 Visualization software multiplies indefinitely an elementary ornamental drawing, taking into account the actual deformation consequent to the adaptation of the cloth on the stuffing (from Morello et al. 2011)

outside the allowed space, at least an error signal should be sent to the operator or, for a perfect simulation, a reaction force applied to his head.

Generally speaking, any object is constrained for displacements and rotations with respect to a local reference frame. These constraints are chosen as process parameters and they should be controlled to stay within allowable limits.

3 D graphics requires an intensive usage of computer memory storage, considering object size, number and real-time refresh. The numerical complexity of the model plays a primary role in determining the refresh speed. To keep this speed at high values, different models of the same part, with different number of details, are generated and contemporarily stored in the computer memory. The operating system selects the most suitable model for the current simulation: detailed models are suitable for close-ups, when few parts are present at the same time in the visible environment, while coarse details are sufficient for viewing from a larger distance, when many parts are to be described. Models change, therefore, with operators motion. In addition, for each exterior surface the quantity of reflected and diffused light must be calculated, as a function of the surface gloss.

Input signals

Input signals regard position and orientation of head and hands of users inside the virtual environment. The user's head position defines the point of view for the virtual environment. This input must be detected at a frequency of 100 Hz at least.

There are four kinds of sensors in use to detect position and orientation of an object in a 3 D space, based upon electromechanical, electromagnetic, acoustic and optic techniques respectively. Electromechanical sensors were the first to be considered; they consist of an articulated arm connected to a helmet worn by the user, leaving adequate freedom to him: The angular displacements of the articulated arm joints allow to calculate the head position and orientation.

Electromagnetic monitoring systems are now more frequently used. A fixed device generates electromagnetic signals that are measured by a set of receivers on the user's head (helmet or stereoscopic glasses). The time delay in receiving the signals is used to calculate the head position and orientation. Acoustic sensors operate in a similar way.

Optical systems are under consideration owing to the performance improvement of processors. Many kinds of sensors are available, from video cameras to optical diodes. Infrared light is particularly suitable because does not interfere with users eyesight.

Position and orientation of the user's hand are used in the virtual environment to input commands to the computer in a more efficient way than with a keyboard or mouse; in particular cases (i.e.: assembling and disassembling simulations, ergonomic evaluation of a vehicle control) these signals are used to move parts of the mathematical model. Particular articulated gloves are used to detect fingers' motion and to apply the correct force feed-back to them.

Interaction with the virtual environment

The correct feeling, received by touching or moving objects, may be reproduced by suitable devices as joysticks with six degrees of freedom (three displacement and three rotations) or interactive gloves. This feeling can be enhanced by including the user's hands in the representation of the virtual environment. The system can detect whether the user's hand can reach and touch any of the virtual objects in the virtual environment. If there is a contact, the system can be programmed to move this part in a consistent direction or to make it integral with the user's hand. If the glove integrates suitable actuators, it is possible to give the user the tactile feeling by the corresponding forces that this object could apply in the real world.

The so called *haptic* technology allows interfacing with the user via the sense of touch, by applying forces, vibrations, and motions to his/her fingers. The word haptic, from the ancient Greek *haptikos*, means pertaining to the sense of touch. This technology contributes to our understanding of how touch and its underlying brain functions work.

An example is shown in Fig. A.25; the user observes the virtual world (in this case the interior of a passenger compartment) through a helmet with binocular display. The seat is a real physical prototype, but the controls are simulated by means of a haptic glove that restores the same feeling the user will have when operating an actual control device. The scene is showing the user while operating a virtual switch on the dashboard, to evaluate ergonomics of this control.

In the future haptic technologies will study a wider range of touch sensations, including the nature of the surface to be touched (smoothness or roughness, temperature, humidity, viscosity, etc.); for the time being, only reaction and inertia forces can be reasonably considered.

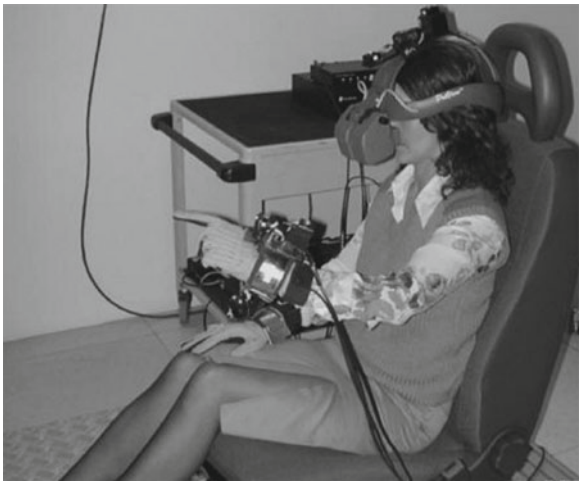

Fig. A.25 The user observes the virtual world (in this case the interior of a passenger compartment) through a helmet with a binocular display. The seat is a real physical prototype; controls are simulated by means of a haptic glove (from Morello et al. 2011)

All haptic devices should obviously be connected to a hand tracking system, to avoid that hands are penetrating into virtual objects, by increasing contact forces significantly. These devices are particularly suitable to investigate the characteristics that are expected of an ideal control or are needed in drive simulators to restore a realistic feeling on the steering wheel.

Visualization devices

Visualization devices may be subdivided into two groups, depending on the technology applied to display the virtual environment: direct vision or projection. The first group includes:

- Head Mounted Displays (HMD), and
- Binocular Omni-Orientation Monitors (BOOM).

With these two systems, the user observes the virtual scenario directly through the internal monitors of the device. An example of HMD is shown in Fig. A.25.

The second group includes the CAVE[2] and the projection backlit walls (Power walls) or tables.

Head mounted displays were the first devices able to allow an immersive experience to the user. They include two miniature displays, like the lenses of a pair of glasses, that simulate the stereoscopic view. A moving tracer on the HMD measures the head position and orientation continuously allowing the computer to calculate consistent views. This device allows more than one user to walk and look around in the virtual environment. The computer processing speed must be high to prevent image slow down or jumps; even if processing speeds dramatically increased, virtual scenes must be simplified to allow the computer to update the images in a realistic way (at least ten times in a second).

BOOM devices contain an optical and display system similar to HMD, but this is contained in a box suspended to an articulated arm, equilibrating its weight. The user looks at the virtual environment through two holes and can explore the space by moving or orienting the device. Suitable sensors control any motion. Devices of both types may be integrated in test rigs, containing also physical parts, such as seats, steering wheel, pedals and shift stick, to study posture comfort, reach of controls, realistic visibility of a car.

Projection based devices consist of special stereoscopic glasses used to observe a semi-transparent screen. The 3 D effect is based upon the fact that each eye sees slightly different images under the perspective they should have in the real world. The human brain interprets these different views to recognize distances and volumes of objects in the environment (stereoscopic view). Stereoscopic glasses separate images perceived by the right and left eye using liquid crystals shutters, synchronized with the actual projection. With suitable infrared pulses sent to the glasses, different projections can be triggered to different eyes.

A typical immersive, non-intrusive projector for virtual reality is the CAVE (Cave Automatic Virtual Environment), a cubic room build up with backlit projection

[2] Power Wall is a registered trade mark of BARCO; CAVE is a registered trade mark of Fakespace.

Fig. A.26 Two pictures of a CAVE including also real elements interfacing the user in a driving simulator (from Morello et al. 2011)

screens, where users can move and interact with the virtual environment. Inside this room, many other devices can be used, such as haptic gloves or joysticks, enhancing user's interaction. Images are projected on the walls, on the ceiling and sometimes also on the floor.

Two pictures of a CAVE including also real elements (haptic pedals and steering wheel) interfacing the user in a drive simulator are shown in Fig. A.26.

If several people are present in a CAVE, or other immersive projection systems, part of them will see the virtual environment from the same point of view as a reference user, irrespective of their actual position. The other problem is that they can cast their shadow on the screen obstructing the view of other users. Also in this case haptic gloves or joysticks can be used.

The main advantages of this device are:

- An ample field of view and a high resolution and
- a work environment accessible to more than one user, with some limitation.

Obvious disadvantages are the space and cost investment required. Power walls offer a cheaper compromise by limiting the projection to a single wall of large dimensions with multiple projectors. Backlit projection tables are suitable to observe spatial phenomena on an object of limited dimensions as a component or a scale model of a vehicle. An example of a virtual wind tunnel, where a computer, solving a mathematical model of the air flow around a vehicle model, can display the shape of the aerodynamic wake, is shown in Fig. A.27. The projection table can be rotated to simulate yaw or pitch to observe their effect on the wake.

Applications to product development

The diffusion of virtual reality has launched a process where many engineering applications of mathematical models convert their outputs, from graphs or printouts, to 3 D models that can be explored and discovered by interacting with them more directly. The success of this approach is due to the higher reproduction fidelity of 3 D outputs that can be observed from any point of view, discovering critical issues that

Fig. A.27 Virtual wind tunnel for scale model of a vehicle (from Morello et al. 2011)

sometimes may be hidden in a conventional printout, representing a plane section made in the wrong place.

For the time being and in the short term, existing mathematical models of virtual reality must be adapted, by developing suitable hardware architectures and visualization software, to enable the simulation and visualization environments to interact correctly at the appropriate synchronization speed. For this reason the applications more often considered in product development regard the interactive visualization of the car exterior and interior for style evaluation, and the digital mock-up exploration for the purposes described previously.

Successful applications can be also mentioned regarding exploring a digital mock-up of virtually crashed or virtually stressed cars; the advantages of virtual reality enable all critical local issues to be grasped quickly. The advantages are demonstrated in practice; in style development, for example, virtual reality applications allow a drastic reduction of the number of physical models required: On occasions they have been reduced from 10 to 2, needed for the final evaluation of two alternatives.

The recent diffusion of virtual reality in product development and research is due to the fact that the best way to evaluate and improve an industrial product is to visualize and use it. This principle also applies to the analysis of performance made by engineers and to perception, acceptance and usability evaluations made by the potential customer.

Virtual reality applications are also starting to spread in multi-sensorial analyses, such as acoustic comfort and human reaction to vehicle controls and displays.

Appendix B
Basics on Vehicle Dynamics

B.1 Mathematical Modelling

The automotive market is increasingly competitive and subjected to an increasing number of standards and rules, primarily regarding safety and environmental impact, issued by regulating bodies and governments and offers its products to more and more demanding customers. While the tasks designers must face become increasingly complex, the time between the conception of a vehicle and its entering the market, the so called *time to market*, is an essential factor for its commercial success. The traditional approach, based on the construction of prototypes, followed by long experimentation and modification phases, is no longer adequate.

The availability of increasingly powerful computational hardware and software gives designers the possibility of predicting the behavior of motor vehicles with increasing precision by using more and more complex and realistic mathematical models with which they can perform detailed numerical experiments. The goal, at present still far from being achieved, is to reduce the importance of physical testing to a simple verification of what virtual testing has ascertained, so that the whole development process can be faster and less expensive, while yielding vehicles of better and better characteristics.

The *mathematical models* on which numerical experimentation is based consist of a number of equations, whose behavior is similar to that of the physical system it replaces. In the case of dynamic models, such as those used to predict the performance of motor vehicles, the model is usually built from a number of ordinary differential equations[3] (ODE).

The complexity of the model depends on many factors, that represent the first choice the analyst has to make. The model must be complex enough to allow a realistic simulation of the system's characteristics of interest, but no more. The more complex the model, the more data it requires, and the more complicated are the solution and interpretation of results. Today it is possible to built very complex

[3] A dynamic model, or a dynamic system, is a model expressed by one or more differential equations containing derivatives with respect to time.

G. Genta et al., *The Motor Car*, Mechanical Engineering Series,
DOI: 10.1007/978-94-007-8552-6, © Springer Science+Business Media Dordrecht 2014

models, but overly complex models yield results from which it is difficult to extract useful insights into the behavior of the system.

Before building the model, the analyst must consider accurately what he wants to obtain from it. If the goal is a good physical understanding of the underlying phenomena, without the need for numerically precise results, simple models are best. If, on the contrary, the aim is precise quantitative results, even at the price of more difficult interpretation, the use of complex models becomes unavoidable.

Finally, it is important to take into account the available data at the stage reached by the project: Early in the definition phase, when most data are still not available, it can be useless to use complex models, into which more or less arbitrary estimates of the numerical values must be introduced. Simplified, or synthetic, models are the most suitable for a preliminary analysis. As the design is gradually defined, new features may be introduced into the model, reaching comprehensive and complex models for the final simulations.

The models of a given vehicle often evolve initially toward a greater complexity, from synthetic models to virtual prototypes, to return later to simpler models. Models are useful not only to the designers in defining the vehicle and its components, but also to test engineers in interpreting the results of testing and performing all adjustments. Simplified models can be used on the test track to allow the test engineers to understand the effect of adjustments and reduce the number of tests required, provided they are simple enough to give an immediate idea of the effect of the relevant parameters. Here the final goal is to adjust the virtual prototype on the computer, transferring the results to the physical vehicle and hoping that at the end of this process only a few validation tests are required.

Simplified models that can be integrated in real time on relatively low power hardware are also useful in control systems. A mathematical model of the controlled system (*plant*, in control jargon) may constitute an *observer* (in the sense of the term used in control theory) and be a part of the control architecture.

The aim of the present appendix is to summarize the basics of mathematical modelling of the dynamic behavior of motor vehicles, showing in particular the synthetic models that are useful in the early stages of vehicle design.

It is possible to demonstrate that under a number of simplifying assumptions the dynamic behavior of any vehicle can be studied by three uncoupled models, dealing with its

- longitudinal behavior,
- lateral behavior (often referred to as handling) and
- vertical behavior (often referred to as comfort).

The basic assumptions that allow this are:

- full linearity of the model, and
- existence of a symmetry plane.

The first assumption implies that the vehicle moves with its longitudinal axis not too removed from the tangent to the trajectory and the steering angles are not too large (i.e. the radius of the trajectory is much larger than the wheelbase), conditions that are

usually verified in the normal use of the vehicle, but not in conditions approaching the limits. Furthermore, the suspension springs and shock absorbers must be linear, and the tires must have a linear behavior in vertical direction. No such assumption is required for the lateral behavior of the tires.

The second assumption is usually verified, at least approximately: except for a few exceptions (motorcycles with a sidecar, some special industrial vehicles) motor vehicles have a vertical plane of symmetry with respect to their shape. The distribution of their internal elements is usually not exactly symmetrical, but this causes a deviation from symmetry that is not too large.

B.2 Reference Frame

The study of the motion of motor vehicles is usually performed with reference to some reference frames that are more or less standardized. They are (Fig. B.1):

- *Earth-fixed axis system XYZ*. This is a right-hand reference frame fixed on the road. It will be regarded as an inertial frame, even if strictly speaking it is not such as it moves along with the Earth, but the inertial effects due to this motion are so small that they can be neglected in all phenomena studied in motor vehicle dynamics. Axes X and Y lie in a horizontal plane while axis Z is vertical, pointing upwards.[4]
- *Vehicle axis system xyz*. This is a right-hand reference frame fixed to the vehicle's center of mass and moving with it. As already stated, if the vehicle has a symmetry plane, the center of mass is assumed to lie in it. The x-axis lies in the symmetry

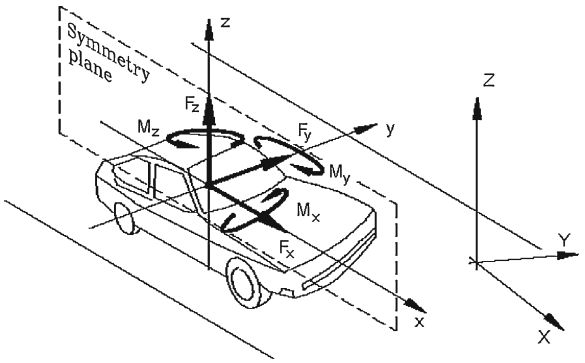

Fig. B.1 Reference frames, forces and moments used for the dynamic study of motor vehicles

[4] Recommendation SAE J670 and ISO/TC 22/SC9 standard state that the Z-axis is vertical and points downwards. In the present text the direction of the Y and Z axes is opposite to that suggested in the mentioned standard.

plane of the vehicle in an almost horizontal direction.[5] The z -axis lies in the symmetry plane, is perpendicular to the x-axis, and points upwards. The y-axis is perpendicular to the other two.[6] The y-axis points to the left of the driver. In the case of vehicles without a symmetry plane, the xz plane is identified by the direction of motion when the wheels are not steered and by a direction perpendicular to the road in the reference position of the vehicle.

B.3 Longitudinal Dynamics

When computing the performance of a vehicle in longitudinal motion (maximum speed, gradeability, fuel consumption, braking, etc.), the vehicle is modelled as a rigid body, or in an even simpler way, as a point mass.

B.3.1 Vehicles as a Point Mass: Resistance to Motion

The presence of suspensions and the compliance of tires are then neglected and the motion is described by a single equation, the equilibrium equation in the longitudinal direction. Assuming that the vehicle moves in the direction of the inertial X-axis, the longitudinal equilibrium equation reduces to

$$m\ddot{X} = \sum_{\forall i} F_{x_i}, \tag{B.1}$$

where F_{x_i} are the various forces acting on the vehicle in the longitudinal direction (aerodynamic drag, rolling resistance, traction, braking forces, etc.).

The rolling resistance of the i-th wheel is assumed, as a first approximation, to be equal to the force pressing the ith wheel against the ground F_{z_i} multiplied by a rolling coefficient f, that depends on many parameters. It is also a function of the speed, and this dependence can be approximated by a quadratic law, so that the rolling resistance can be expressed as

$$R_r = \sum_{\forall i} F_{z_i} \left(f_0 + K V^2 \right). \tag{B.2}$$

[5] The mentioned standard states that the x-axis is contained in the plane of symmetry of the vehicle, is "substantially" horizontal and points forward.

[6] Here again there is a deviation from the mentioned standards.

Assuming that the rolling coefficient is the same for all wheels,[7] it can be brought out from the sum. The sum of the forces perpendicular to the ground on a road with a longitudinal grade angle α, taking into account aerodynamic lift $F_{z_{aer}}$, is

$$\sum_{\forall i} F_{z_i} = \left[mg\cos(\alpha) - F_{z_{aer}}\right] = \left[mg\cos(\alpha) - \frac{1}{2}\rho V_r^2 S C_z\right], \tag{B.3}$$

where the usual expression for the aerodynamic forces has been used. In this expression, ρ is the air density, V_r is the velocity with respect to the air (it is equal to the vehicle speed V when there is no wind, S is a reference surface (usually the area of the cross section of the vehicle) and C_z is a coefficient that depends on the Reynold's and Mach numbers, but is considered as approximately constant. Thus it follows that

$$R_r = \left[mg\cos(\alpha) - \frac{1}{2}\rho V_r^2 S C_z\right](f_0 + K V^2). \tag{B.4}$$

Aerodynamic drag (or, better, the aerodynamic force in the x direction) is expressed by a formula similar to that of force in z direction:

$$R_a = \frac{1}{2}\rho {V_r}^2 S C_x \tag{B.5}$$

where also C_x is a coefficient that depends on the Reynold's and Mach numbers, but is considered as approximately constant

With increasing speed, the importance of the aerodynamic drag grows and at a given value of the speed it becomes more important than rolling resistance. This speed is lower for small cars while for larger vehicles, particularly for trucks at full load, the rolling resistance is the primary form of drag. Another factor is that usually the mass of the vehicle grows with its size more rapidly than the area of its cross section.

If the road is not level, the component of weight acting in a direction parallel to the velocity V, i.e. the grade force

$$R_g = mg\sin(\alpha) \tag{B.6}$$

must be added to the resistance to motion.

The grade force becomes far more important than all other forms of drag even for moderate values of grade. The total resistance to motion, or road load, as it is commonly referred to, can be written in the form

$$R = \left[mg\cos(\alpha) - \frac{1}{2}\rho V^2 S C_z\right](f_0 + K V^2) + \frac{1}{2}\rho V^2 S C_x + mg\sin(\alpha), \tag{B.7}$$

[7] This assumption holds only as a first approximation, since it does not take into account the dependence of f on the driving or braking conditions or other variables.

where, assuming that the air is still, the velocity with respect to air V_r becomes conflated with velocity V.

To highlight its dependence on speed, the road load can be written as

$$R = A + BV^2 + CV^4, \tag{B.8}$$

where

$$A = mg\,[f_0 \cos(\alpha) + \sin(\alpha)],$$

$$B = mgK\cos(\alpha) + \frac{1}{2}\rho S[C_x - C_z f_0],$$

$$C = -\frac{1}{2}\rho S K C_z.$$

The last term in Eq. (B.8) becomes important only at very high speed in the case of vehicles with strong (negative) lift: It is usually neglected except for racing cars.

Since the grade angle of roads open to vehicular traffic is usually not large, it is possible to assume that

$$\cos(\alpha) \approx 1, \quad \sin(\alpha) \approx \tan(\alpha) \approx i,$$

where i is the grade of the road. In this case coefficient B is independent of the grade of the road and

$$A \approx mg(f_0 + i)$$

depends linearly on it. C never depends on the grade.

B.3.2 Power Needed For Motion

The power needed to move at constant speed V is obtained simply by multiplying the road load given by Eq. (B.8) by the value of the velocity

$$P_n = VR = AV + BV^3 + CV^5. \tag{B.9}$$

Motion at constant speed is possible only if the power available at the wheels at least equals the required power. This means that the engine must supply sufficient power, taking into account losses in the transmission as well, and that the road-wheel contact must be able to transmit this power.

The engine drives the wheels through a mechanical transmission whose task is essentially that of reducing the angular velocity of the engine to that required at the wheels. If a reciprocating internal combustion engine is used, the transmission also

has the task of uncoupling the engine from the wheels at a stop or at low speed, for which reason the driveline includes a clutch or a torque converter as well.

It is possible, at least as a first approximation, to state a value of the efficiency η_t for any type of driveline. The power available at the wheels is thus

$$P_a = P_e \eta_t. \tag{B.10}$$

Depending on the type of transmission, the efficiency can be considered as a constant (obviously only as a first approximation), or may be computed as a function of several parameters, but only after assessing the working conditions of the driveline and above all of the torque converter, if present.

The equation linking the speed of the engine Ω_e to that of the wheels is simply

$$V = \Omega_e R_e \tau_t, \tag{B.11}$$

where τ_t is the overall gear ratio , defined as the ratio between the speed of the wheels and that of the engine shaft, and is usually smaller than 1. Once the gear ratios of all parts of the transmission are known, the power available at the wheels can be plotted as a function of the speed of the vehicle on the same plot where the power needed for motion at constant speed is reported.

If the curves of the required and available power are plotted on a logarithmic plot, any change of the gear ratio causes a translation of the curves along the V-axis, while a change in the efficiency of the driveline causes a translation of the curve related to the available power along the P-axis (Fig. B.2a. If a continuous transmission (CVT) is present, the position of the latter curve is a function of the gear ratio, and then it is possible to define a zone on the VP-plane where all possible working conditions are included.

B.3.3 Maximum Speed

The maximum speed that can be reached on level road with a given transmission ratio can be found by intersecting the curve of the available power at the wheels with that of the required power on level road. The transmission ratio causing this intersection to occur at the maximum available power allows the vehicle to reach the highest speed that can be attained by a given vehicle-engine combination (curve 1 in Fig. B.2b).

The computation of the maximum speed and of the overall gear ratio τ_t required to reach it is straightforward. By intersecting the required power curve with the horizontal straight line

$$P = P_{a_{max}} = P_{e_{max}} \eta_t,$$

a fifth degree equation is obtained

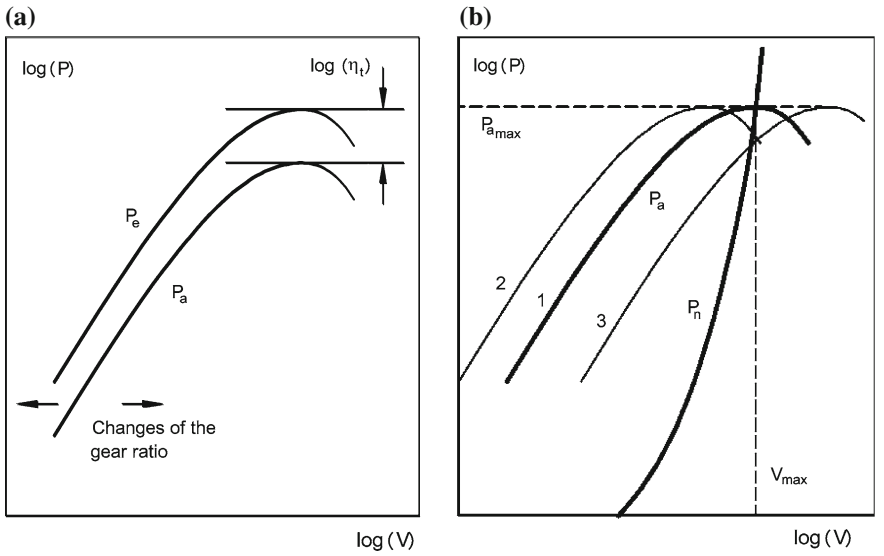

Fig. B.2 (**a**): Curves of maximum engine power and power available at the wheels plotted with logarithmic scales. Changing the efficiency of the transmission and the overall transmission ratio. (**b**): Maximum speed for a vehicle with internal combustion engine

$$AV + BV^3 + CV^5 = P_{e_{max}}\eta_t, \tag{B.12}$$

whose solution directly yields the maximum value of the speed.

If aerodynamic lift is neglected (actually it is sufficient to neglect the contribution to rolling resistance proportional to the square of the speed due to lift), C vanishes and the equation is cubic. Its solution can be obtained in closed form

$$V_{max} = A^* \left(\sqrt[3]{B^* + 1} - \sqrt[3]{B^* - 1} \right), \tag{B.13}$$

where

$$A^* = \sqrt[3]{\frac{P_{e_{max}}\eta_t}{2mgK + \rho S C_X}} = \sqrt[3]{\frac{P_{e_{max}}\eta_t}{2B}},$$

$$B^* = \sqrt{1 + \frac{8m^3 g^3 f_0^3}{27 P_{m_{max}}^2 \eta_t^2 (2mgK + \rho S C_X)}} = \sqrt{1 + \frac{4A^3}{27 P_{m_{max}}^2 \eta_t^2 B}}.$$

Once the maximum speed has been obtained, the gear ratio allowing the vehicle to reach it is

$$\tau_t = \frac{V_{max}}{R_e (\Omega_e)_{P_{max}}}, \tag{B.14}$$

where $(\Omega_e)_{P_{max}}$ is the engine speed at which the peak power is obtained.

If the transmission is of the mechanical type, the overall gear ratio is the product of the gear ratio at the gearbox τ_g (in the relevant gear) and that of the final drive τ_f

$$\tau_t = \tau_g \tau_f .$$

The transmission ratio of the gearbox, which in top gear is usually close to 1, can be stated and consequently the gear ratio τ_f at the final drive can be computed.

Note that this procedure is based on the assumption that the intersection in Fig. B.2 occurs at the peak of the engine power curve. This can, however, occur in only one given condition, since not only the load, but also the rolling resistance coefficient and even the air density, affect the road load curve. Air density also affects the engine power curve. If the intersection occurs in the descending branch of the curve (situation 2 in Fig. B.2) the vehicle is said to be "undergeared", i.e., the overall transmission ratio is "too short". Conversely, if the intersection occurs in the ascending branch of the curve (situation 3 in Fig. B.2), the vehicle is "overgeared " and the overall transmission ratio is "too long".

There are thus two ways of choosing the top gear ratio: One has already been stated, namely a "fast" gear ratio, chosen in order to reach the maximum speed. A different approach is to use a longer overgeared ratio, with the goal of reducing fuel consumption (see below). In practical terms, this trade-off is typical of five or six speed transmissions: Either the maximum speed is reached in fifth (sixth) gear or in fourth (fifth) gear, the longest one being an overdrive gear.

This strategy works only in the case of vehicles with high power/weight ratio: In low powered vehicles, this "economy" gear would be difficult to use since any increase of the required power, e.g. due to a slight grade, headwind, etc., would compel a shift to a shorter gear. Undergearing may be a necessity in this case.

B.3.4 Gradeability

The maximum grade that can be managed with a given gear ratio may be obtained by plotting the curves of the required power at various values of the slope and looking for the curve that is tangent to the curve of the available power (Fig. B.3). The slope so obtained is, however, only a theoretical result, since it can be managed only at a single value of the speed: If the vehicle travels at a higher speed, it slows down because the power is not sufficient, but if its speed is reduced the power is insufficient and the vehicle slows down further: The condition is therefore unstable and the vehicle stops.

To be able to manage a specified slope safely, the curve of the available power must be above that of the required power in a whole range of speeds, starting from a value low enough to assure that starting on that slope is possible. To choose a value of the gear ratio of the bottom gear allowing the vehicle to start on a given grade,

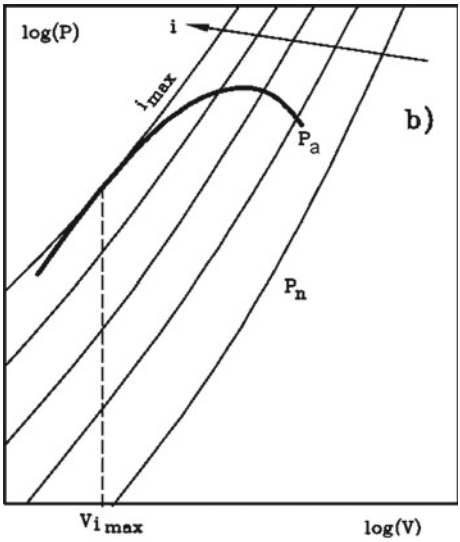

Fig. B.3 Maximum slope for a vehicle with internal combustion engine

it is possible to state a reference speed and to compute the gear ratio in such a way that at that speed the P_a and P_n curves intersect.

As the vehicle is moving at low speed, only the first term of the required power curve needs to be accounted for. As the power developed by the engine can be written in the form

$$P_e = M_e \Omega_e = M_e \frac{V}{R_e \tau_g \tau_f}, \tag{B.15}$$

where M_e is the engine torque, the equilibrium condition allows the overall gear ratio to be computed as

$$\tau_t = \frac{M_e \eta_t}{R_e m g [f_0 \cos(\alpha) + \sin(\alpha)]}. \tag{B.16}$$

The value of the engine torque to be introduced into Eq. (B.16) can be the maximum torque available at the minimum engine speed, possibly multiplied by a number smaller than 1 for safety. The mass of the vehicle must be that at full load, including the maximum trailer mass the vehicle is allowed to tow. For the grade, values of 25 % or even 33 % for road vehicles can be considered, but it must be kept in mind that in some cases, as in ferry ramps or private garage ramps, very steep grades may be encountered.

Another consideration in the choice of the gear ratio for the bottom gear is to assure a regular working of the engine at a speed chosen so as to avoid a prolonged use of the clutch in low speed driving. A reference value may be 6 or 8 km/h. Both criteria must be satisfied. Once the ratios of the bottom and top gears have been chosen, the intermediate ones can be stated using different criteria. The simplest is to set them in geometric sequence, i.e., stating that the ratios between two subsequent

gear ratios are all equal. Operating in this way, the available power curves on the $P(V)$ logarithmic plot are all equispaced.

B.3.5 Fuel Consumption at Constant Speed

The energy needed to travel at constant speed can be immediately computed by multiplying the power required for constant speed driving by the time

$$e = P_n t = \frac{P_n d}{V}, \tag{B.17}$$

where d is the distance travelled. Note that Eq. (B.17) gives the energy required at the wheels: To obtain the energy actually required, it must be divided by the various efficiencies (transmission, engine, etc.).

If the efficiency of the engine η_e and the thermal value H of the fuel are known, the fuel consumption can be computed. Introducing the expression derived from Eq. (B.7) for the total road load into the expression for the power, the fuel consumption per unit distance Q is

$$Q = \frac{A + BV^2 + CV^4}{\eta_t \eta_e H \rho_f}, \tag{B.18}$$

where ρ_f is the density of the fuel, introduced to obtain the consumption in terms of volume of fuel per unit of distance. In S.I. units it is measured in m^3/m, while liters per 100 km is a more practical, although not consistent, unit. Often the reciprocal of Q, expressed in km per liter or miles per gallon, is used.

To compute the consumption Q, the simplest procedure is to obtain the power required at the wheels as a function of the speed and hence to compute the power the engine must supply to travel at constant speed

$$P_e = \frac{P_n}{\eta_t}.$$

Once the transmission ratio has been stated, the rotational speed of the engine is known and thus the working point on the map of the engine is located. From it the efficiency η_e or, which is the same, the specific fuel consumption

$$q = \frac{H}{\eta_e}$$

is obtained and the fuel consumption can be computed as

$$Q = \frac{q P_n}{\eta_t V \rho_f}. \tag{B.19}$$

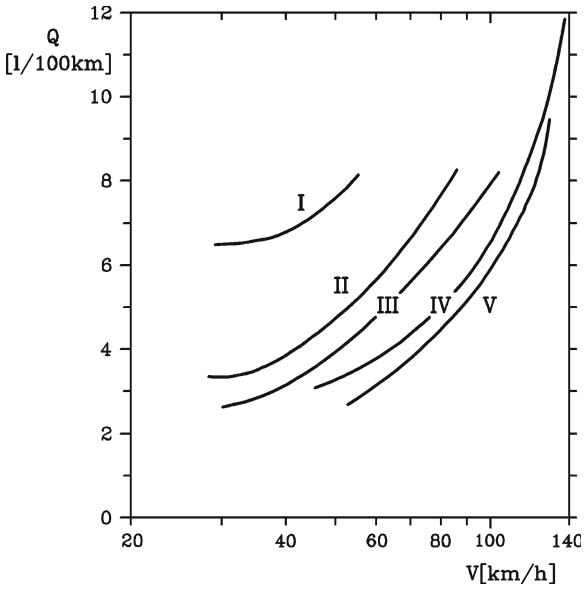

Fig. B.4 Fuel consumption with different gear ratios at constant speed on level road. Passenger vehicle with a five-speed gearbox

The curves $Q(V)$ are of the type shown in Fig. B.4. They usually have a minimum at low speed, obtained in conditions in which the engine works at low power with low efficiency. Since the conditions in which the engine works depend on the overall transmission ratio, the fuel consumption is also largely influenced by the value of the gear ratio. Usually the longer the ratio, the lower the consumption, as a "long" ratio allows the engine to be used at low speed in conditions which are close to the maximum power, where the specific fuel consumption is low.

B.3.6 Acceleration

If the curve of the required power lies, at a certain speed, below that of the power available at the wheels, the difference $P_a - P_n$ between the two is the power available to accelerate the vehicle .

Consider a vehicle with a mechanical transmission with a number of different gear ratios. During acceleration a number of rotating elements (wheels, transmission, the engine itself) must increase their angular velocity, and it is expedient to write an equation linking the engine power with the kinetic energy $\mathcal{T}$ of the vehicle

$$\eta_t P_e - P_n = \frac{d\mathcal{T}}{dt} \,. \tag{B.20}$$

The transmission efficiency should not be included for the part or the engine power needed to accelerate the engine, but the error so introduced is usually negligible.

Once the transmission ratio has been chosen, Eq. (B.11) gives the relationship between the speed of the vehicle and the rotational speed of the engine. Similar relationships may be used for the other rotating elements that must be accelerated when the vehicle speeds up.

The kinetic energy of the vehicle can thus be expressed as

$$\mathcal{T} = \frac{1}{2} m V^2 + \frac{1}{2} \sum_{\forall i} J_i \Omega_i^2 = \frac{1}{2} m_e V^2, \tag{B.21}$$

where the sum extends to all rotating elements which must be accelerated when the vehicle speeds up. The term m_e is the equivalent or apparent mass of the vehicle, i.e., the mass of an object that, when moving at the same speed as the vehicle, has the same total kinetic energy. Usually it is written in the form

$$m_e = m + \frac{J_w}{R_e^2} + \frac{J_t}{R_e^2 \tau_f^2} + \frac{J_e}{R_e^2 \tau_f^2 \tau_g^2}, \tag{B.22}$$

where J_w is the total moment of inertia of the wheels, which are assumed to have the same radius and hence to rotate at the same speed, and of all elements rotating at their speed, J_t is the moment of inertia of the propeller shaft and of all elements of the transmission, and J_e is the moment of inertia of the engine, the clutch and all the elements rotating at speed Ω_e.

To account for the fact that the engine is accelerated directly, at least in an approximate way, the last term is sometimes multiplied by η_t. The modifications to Eq. (B.22) to take the presence of different wheels on different axles into account are obvious.

Of the three latter terms, the first is usually small, the second negligible, while the third may become important, particularly in low gear. As only the last term depends on the transmission ratio at the gearbox, the equivalent mass can be written in the form

$$m_e = F + \frac{G}{\tau_g^2}, \tag{B.23}$$

where

$$F = m + \frac{J_w}{R_e^2} + \frac{J_t}{R_e^2 \tau_f^2}, \quad G = \frac{J_e}{R_e^2 \tau_f^2}$$

or, possibly,

$$G = \frac{J_e \eta_t}{R_e^2 \tau_f^2}.$$

As the equivalent mass is a constant, once the gear ratio has been chosen, Eq. (B.20) yields

$$\eta_t P_e - P_n = m_e V \frac{dV}{dt}. \tag{B.24}$$

From Eq. (B.24), the maximum acceleration the vehicle is capable of at various speeds is immediately obtained

$$\left(\frac{dV}{dt}\right)_{max} = \frac{\eta_t P_e - P_n}{m_e V}, \tag{B.25}$$

where the engine power P_e is the maximum power the engine can deliver at the speed Ω_e, corresponding to speed V.

The minimum time needed to accelerate from speed V_1 to speed V_2 can be computed by separating the variables in Eq. (B.25)

$$dt = \frac{m_e V dV}{\eta_t P_e - P_n} \tag{B.26}$$

and integrating

$$T_{V_1 \to V_2} = \int_{V_1}^{V_2} \frac{m_e}{\eta_t P_e - P_n} V dV. \tag{B.27}$$

The integral must be performed separately for each velocity range in which the equivalent mass is constant, i.e. the gearbox works with a fixed transmission ratio. Although it is possible to integrate Eq. (B.27) analytically if the maximum power curve is a polynomial, numerical integration is usually performed.

A graphical interpretation of the integration is shown in Fig. B.5 : The area under the curve

$$\frac{V m_e}{\eta_t P_e - P_n} = \frac{1}{a}$$

versus V is the time required for the acceleration.

The speeds at which gear shifting must occur to minimize the acceleration time are readily identified on the plot $1/a(V)$. Since the area under the curve is the acceleration time or the time to speed, the area must be minimized and gears must be shifted at the intersection of the various curves. If they do not intersect, the shorter gear must be used up to the maximum engine speed.

B.3.7 Braking

The study of braking on straight road is performed using Eq. (B.1). Apart from cases in which the vehicle is slowed by the braking effect of the engine, which can dissipate a non-negligible power, and by regenerative braking in electric and hybrid vehicles, braking is performed in all modern vehicles on all wheels. Subscript i thus extends to

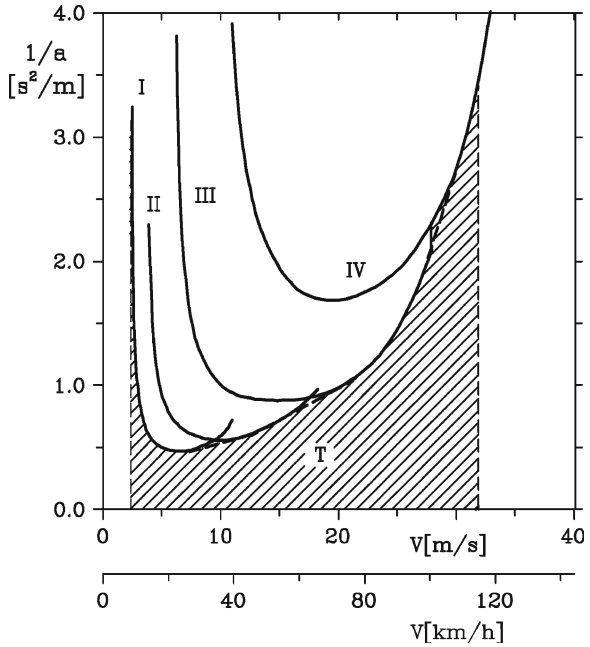

Fig. B.5 Function $1/a(V)$ showing the optimum speeds for gear shifting. The hatched area is the time to speed

all wheels or, when thinking in terms of axles, as is usual for motion in symmetrical conditions, on all axles.

Ideal braking can be defined as the condition in which all wheels brake with the same longitudinal force coefficient μ_x, defined as the ratio between the longitudinal force a wheel is exerting and the forcing loading it on the road.

The study of braking forces the vehicle can exert follows the same scheme seen in the previous section, the only obvious difference being that braking forces, like the corresponding longitudinal force coefficients and the longitudinal slip, are negative. The acceleration can thus be computed as

$$\ddot{X} = \frac{dV}{dt} = \frac{1}{m} \sum_{\forall i} \mu_{x_i} F_{z_i}, \tag{B.28}$$

remembering that when braking both the longitudinal force coefficient and the acceleration are negative.

The longitudinal equation of motion of the vehicle is thus

$$\frac{dV}{dt} = \frac{\sum_{\forall i} \mu_{x_i} F_{z_i} - \frac{1}{2}\rho V^2 S C_X - f \sum_{\forall i} F_{z_i} - mg \sin(\alpha)}{m}, \tag{B.29}$$

where m is the actual mass of the vehicle and not the equivalent mass, and α is positive for uphill grades. The rotating parts of the vehicle are slowed down directly by the brakes, and hence do not enter into the evaluation of the forces exchanged between vehicle and road. They must be accounted for when assessing the required braking power of the brakes and the energy that must be dissipated.

Aerodynamic drag and rolling resistance can be neglected in a simplified study of braking, since they are usually far smaller than braking forces. Also, rolling resistance can be considered as causing a braking moment on the wheel more than a direct braking force on the ground.

Since in ideal braking all force coefficients μ_{x_i} are assumed to be equal, the deceleration is

$$\frac{dV}{dt} = \mu_x \left[g\cos(\alpha) - \frac{1}{2m}\rho V^2 S C_Z \right] - g\sin(\alpha). \tag{B.30}$$

On level road, for a vehicle with no aerodynamic lift, Eq. (B.30) reduces to

$$\frac{dV}{dt} = \mu_x g. \tag{B.31}$$

The maximum deceleration in ideal conditions can be obtained by introducing the maximum negative value of μ_x into Eq. (B.30) or (B.31). The assumption of ideal braking implies that the braking torques applied on the various wheels are proportional to the forces F_z, if the radii of the wheels are all equal. This may occur in only one condition, unless some sophisticated control device is implemented to allow braking in ideal conditions.

In general, it is possible to define an efficiency of braking η_b as the ratio between the acceleration obtained in actual conditions and that occurring in ideal conditions, so that the actual deceleration on level road is

$$\frac{dV}{dt} = \eta_b \mu_x g. \tag{B.32}$$

The efficiency of braking η_b is obviously smaller than 1 and depends on many factors, like the road conditions and the force the driver exerts on the brakes.

The brakes cannot dissipate the kinetic energy of the vehicle directly; they usually work as a heat sink, storing some of the energy in the form of thermal energy and dissipating it in due time. Care must obviously be exerted to design the brakes in such a way that they can store the required energy without reaching excessively high temperatures and so that adequate ventilation for cooling is ensured. The average value of the braking power must, at any rate, be lower than the thermal power the brakes can dissipate.

B.4 Lateral Dynamics (Handling)

To steer a wheeled vehicle the driver operates the steering wheel causing some wheels to work with a sideslip and to generate lateral forces. These forces cause a change of attitude of the vehicle (the attitude or sideslip angle β is defined as the angle between the longitudinal direction of the vehicle and the velocity vector, see Fig. B.6) and then a sideslip of all wheels: The resulting forces bend the trajectory. However, the linearity of the behavior of the tires, at least for small sideslip angles, the high value of the cornering stiffness and the short time delay with which the wheels respond to changes in the sideslip and camber angles, give the driver the impression of a kinematic steering, i.e. that the wheels are in pure rolling, without any sideslip, and the trajectory seems to be determined by the directions of the midplanes of the wheels.

This impression has influenced the study of the handling of wheeled vehicles for a long time, originating the very concept of kinematic steering and in a sense hiding the true meaning of the relevant phenomena. Actually, the concept of kinematic steering was applied first to horse drawn wagons: Ackermann patented in 1818 the idea that the lines perpendicular to the midplanes of the wheels passing through the contact points on the ground should converge in the instant center of rotation of the vehicle.[8] This concept worked well in connection with carriage wheels provided with steel tires and later was applied to motor vehicles. Only in the 1930s did some experiments show the importance of the sideslip angle in generating lateral forces and this concept was finally formalized by Olley in 1937.

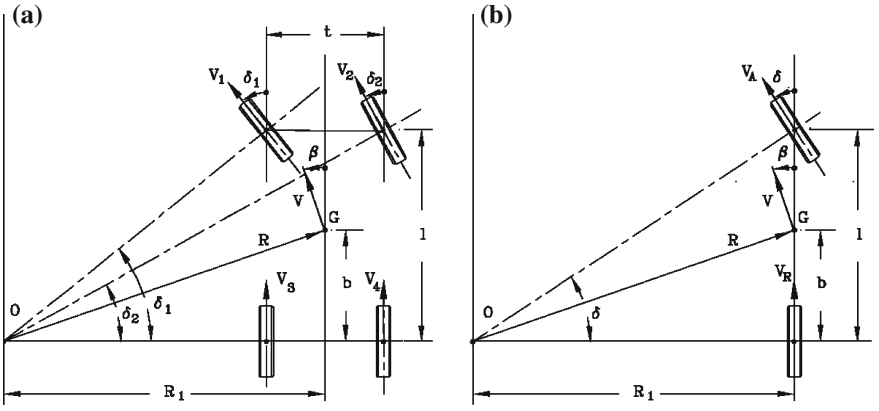

Fig. B.6 Kinematic steering of a four-wheeled and a two-wheeled vehicle

[8] Erasmus Darwin had actually this idea in 1758 but the one who applied it first was a German carriage builder who, in 1818, had his agent in England, Rudolph Ackermann, patent what is now called the Ackermann steering geometry.

The impressions received by the driver are in good accordance with the kinematic approach, at least for all the linear part of the behavior of the tire. When high values of the sideslip angles are reached, the average driver has the impression of losing control of the vehicle, much more so if this occurs abruptly. This impression is confirmed by the fact that in normal road conditions, particularly if radial tires are used, the sideslip angles become large only when approaching the limit lateral forces.

B.4.1 Kinematic Steering

Low speed or kinematic steering is, as already stated, defined as the motion of a wheeled vehicle determined by pure rolling of the wheels. The velocities of the centres of all the wheels lie in their midplane or, in other words, the sideslip angles α_i are vanishingly small. In this condition, the wheels cannot exert any cornering force to balance the centrifugal force due to the curvature of the path. Kinematic steering is thus possible only if the velocity is vanishingly small.

Consider a vehicle with four wheels, two of which can steer (Fig. B.6). The relationship that must be verified to allow kinematic steering is easily found, by imposing that the perpendiculars to the midplanes of the front wheels meet the ones of the rear wheels in the same point:

$$\tan(\delta_1) = \frac{l}{R_1 - \frac{t}{2}}, \qquad \tan(\delta_2) = \frac{l}{R_1 + \frac{t}{2}}. \tag{B.33}$$

By eliminating R_1 between the two equations, a direct relationship between δ_1 and δ_2 is readily found:

$$\cot(\delta_1) - \cot(\delta_2) = \frac{t}{l}. \tag{B.34}$$

A device allowing steering of wheels in exact compliance with Eq. (B.34), is usually referred to as *Ackerman steering* or *Ackerman geometry*. No actual steering mechanism allows one to follow such a law exactly and a *steering error* $\Delta\delta_2$, defined as the difference between the actual value of δ_2 and that obtained from Eq. (B.34) can be obtained as a function of δ_1.

The radius of the trajectory of the centre of mass of the vehicle is:

$$R = \sqrt{b^2 + R_1^2} = \sqrt{b^2 + l^2 \cot^2(\delta)}, \tag{B.35}$$

where δ is the steering angle of the equivalent two-wheeled vehicle (Fig. B.6b), also called *monotrace* model. Although it should be computed by averaging the cotangents of the angles of the two wheels, it is very close to the direct average of the angles.

In case the radius of the trajectory is large if compared to the wheelbase of the vehicle, Eq. (B.35) reduces to:

$$R \approx l \cot(\delta) \approx \frac{l}{\delta}. \tag{B.36}$$

Equation (B.36) can be rewritten in the form:

$$\frac{1}{R\delta} \approx \frac{1}{l}. \tag{B.37}$$

The expression $1/R\delta$ has an important physical meaning: It is the ratio between the response of the vehicle, in terms of curvature $1/R$ of the trajectory, and the input which causes it. It is therefore a sort of transfer function for the directional control and can be referred to as *trajectory curvature gain* . In kinematic steering conditions it is equal to the reciprocal of the wheelbase.

B.4.2 Ideal Steering

If the speed is not vanishingly small, the wheels must move with suitable sideslip angles to generate cornering forces. A simple evaluation of the steady-state steering of a vehicle in high-speed or dynamic steering conditions may be performed as follows. Consider a rigid vehicle moving on level road with transversal slope angle α_t and neglect the aerodynamic side force. Define a η-axis parallel to the road surface, passing through the centre of mass of the vehicle and intersecting the vertical for the centre of the path, which in steady-state condition is circular (Fig. B.7). Axis η does not coincide with the y axis, except at one particular speed.

Assume that the road is flat and neglect aerodynamic forces. The equilibrium equation in η direction can be written by equating the centrifugal force mV^2/R to the sum of the forces P_η due to the tires

$$\frac{mV^2}{R} = \sum_{\forall i} P_{\eta_i}. \tag{B.38}$$

For a first approximation study, forces P_η may be conflated with the cornering forces F_y of the tires and all wheels may be assumed to work with the same side force coefficient μ_y. Since the last assumption is similar to that seen for braking in ideal conditions, this approach will be referred to as *ideal steering*. These two assumptions lead to substituting the expression $\sum_{\forall i} P_{\eta_i}$ with $\mu_y F_z$.

Force F_z exerted by the vehicle on the road is

$$F_z = \sum F_{z_i} = mg. \tag{B.39}$$

By introducing Eq. (B.39) into Eq. (B.38) the ratio between the lateral acceleration and the gravitational acceleration g is

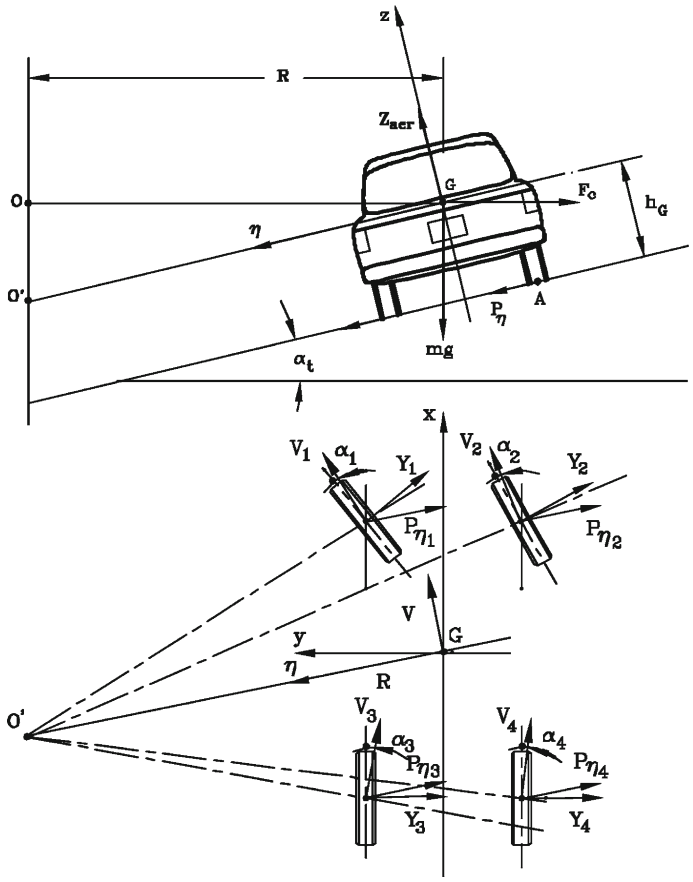

Fig. B.7 Simplified model for dynamic steering

$$\frac{V^2}{Rg} = \mu_y. \tag{B.40}$$

By introducing the maximum value of the side force coefficient μ_{y_p} into Eq. (B.40), it is possible to obtain the maximum value of the lateral acceleration

$$\left(\frac{V^2}{R}\right)_{max} = g\mu_{y_p}. \tag{B.41}$$

The maximum speed at which a bend with radius R can be negotiated is

$$V_{max} = \sqrt{Rg}\sqrt{\mu_{y_p}}. \tag{B.42}$$

The limitation to the maximum lateral acceleration due to the cornering force that the tires can exert is, however, not the only limitation, at least theoretically. Another can come from the danger of rollover occurring if the resultant of forces in the yz plane crosses the road surface outside point A (Fig. B.7).

The moment of the forces applied to the vehicle in the ηz-plane about point A is

$$M_A = -\frac{t}{2} mg + h_G \frac{mV^2}{R}. \tag{B.43}$$

The limit condition for rollover can then be computed by equating moment M_A to zero,

$$\left(\frac{V^2}{R}\right)_{max} = g\frac{t}{2h_G}. \tag{B.44}$$

The rollover condition is identical to the sliding conditions, once ratio $\frac{t}{2h_G}$ has been substituted for μ_{y_p}.

The maximum lateral acceleration is thus

$$\left(\frac{V^2}{R}\right)_{max} = g \min\left\{\mu_{y_p}, \frac{t}{2h_G}\right\}. \tag{B.45}$$

Whether the limit condition first reached is that related to sliding, with subsequent spin out of the vehicle, or related to rolling over depends on the relative magnitude of μ_{y_p} and $\frac{t}{2h_G}$. If the former is smaller than the latter, as often occurs, the vehicle spins out. This condition can be written in the form

$$\mu_{y_p} < \frac{t}{2h_G}.$$

If a negative aerodynamic lift is present, like in racing cars, at high speed strong lateral accelerations are possible. Also a transversal slope of the road may have a large effect on the lateral acceleration.

The value of μ_{y_p} at which rollover may occur is as high as $1.2 \div 1.7$ for sports cars, $1.1 \div 1.6$ for saloon cars, $0.8 \div 1.1$ for pickup and vans and $0.4 \div 0.8$ for heavy and medium trucks. Only in the latter case does rollover seem to be a possibility, at least if the lateral forces acting on the vehicle are restricted to the cornering forces of the tires.

This model is only a rough approximation of the actual situation, as it is based on the assumption that the side force coefficients μ_y of all wheels are equal, implying that all wheels work with the same sideslip angle α. It also ignores the effect of the different directions of the cornering forces of the various wheels, which should be considered as perpendicular to the midplanes of the wheels and not directed along the η axis. The load transfer between the wheels of the same axle and the presence of the suspensions have also been neglected, two other assumptions contributing to the lack of precision of this model.

If the maximum speed at which a circular path can be negotiated is measured in a steering pad test and the value of the lateral force coefficient is computed through Eq. (B.42), a value of μ_{y_p} well below that obtained from tests on the tires is obtained.

The cornering force coefficient obtained in this way is that of the vehicle as a whole, and the difference between its value and that related to the tires gives a measure of how well the vehicle is able to exploit the cornering characteristics of its wheels.

The side force coefficient measured on the whole vehicle also depends on the radius of the path, with a decrease on narrow bends. The majority of industrial and passenger vehicles are able to use only a fraction, from 50 to 80 %, of the potential cornering force of the tires, with higher values found only in sports cars. This reduction of the lateral forces makes the danger of rollover even more remote.

Actually, rolling over in a quasi-static condition is impossible for most vehicles, notwithstanding the fact that rollover actually occurs in many road accidents. Rollover can usually be ascribed to dynamic phenomena in nonstationary conditions or to lateral forces caused by side contacts, e.g. of the wheels with the curb, that rule out the possibility of side slipping while causing far stronger lateral forces to be exerted on the wheels. Moreover, the presence of the suspensions makes rollover a likely outcome of many accidents.

B.4.3 High-Speed Cornering: Simplified Approach

To go beyond the extremely simplified model of ideal steering, the distribution of cornering forces between the axles, the sideslip angle of the vehicle on its path and the sideslip angles of the wheels must be taken into account .

Assume that the vehicle is moving at constant speed on a circular path and that the road is level. Moreover, assume that the radius of the path R is much larger than the wheelbase l and, as a consequence, all sideslip angles are small. The small size of all angles allows the "monotrack" or "bicycle" model to be used . Neglecting aerodynamic forces and aligning torques of the wheels, the forces acting in the xy plane at the tire-road interface are shown in Fig. B.8.

The equilibrium equation in the direction of the y axis is similar to Eq. (B.38), except for the presence of the sideslip and steering angles

$$\frac{mV^2}{R}\cos(\beta) = \sum_{\forall i} F_{x_i}\sin(\delta_i) + \sum_{\forall i} F_{y_i}\cos(\delta_i). \tag{B.46}$$

The equilibrium to rotations about point G can be expressed as

$$\sum_{\forall i} F_{x_i}\sin(\delta_i)x_i + \sum_{\forall i} F_{y_i}\cos(\delta_i)x_i = 0. \tag{B.47}$$

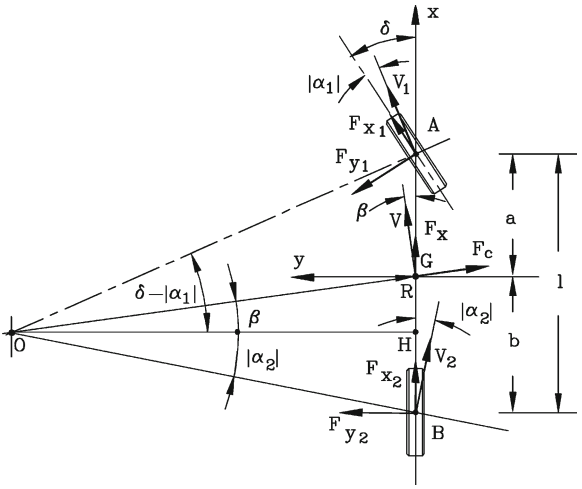

Fig. B.8 Simplified model (monotrack vehicle) for studying the handling of a two-axle vehicle

Since angles β and δ_i are assumed to be small, the terms containing the longitudinal forces of the tires can be neglected and the equilibrium equations reduce to

$$\begin{cases} \sum_{\forall i} F_{y_i} = \frac{mV^2}{R} \\ \sum_{\forall i} F_{y_i} x_i = 0. \end{cases} \tag{B.48}$$

For a two-axle vehicle, they can be immediately solved, yielding

$$F_{y_1} = \frac{mV^2}{R}\frac{b}{l}, \quad F_{y_2} = \frac{mV^2}{R}\frac{a}{l}. \tag{B.49}$$

When the sideslip angles of the wheels are small, the lateral forces (cornering forces) of the axles can be assumed to be proportional to the sideslip angles α_i through their cornering stiffness C_i. As a consequence, it follows that

$$\alpha_i = -\frac{F_{y_i}}{C_1}, \tag{B.50}$$

i.e.

$$\alpha_1 = -\frac{mV^2}{R}\frac{b}{lC_1}, \quad \alpha_2 = -\frac{mV^2}{R}\frac{a}{lC_2}. \tag{B.51}$$

The cornering stiffness of the axles is equal to the cornering stiffness of the wheels multiplied by the number of wheels of the axle.

A relationship between the sideslip and steering angles can be found with simple geometrical considerations from Fig. B.8,

$$\delta - \alpha_1 + \alpha_2 = \frac{l}{R}. \tag{B.52}$$

Introducing the expressions of the sideslip angles into Eq. (B.52), it follows that

$$\delta = \frac{l}{R} + \frac{mV^2}{Rl}\left(\frac{b}{C_1} - \frac{a}{C_2}\right), \tag{B.53}$$

or, in terms of path curvature gain ,

$$\frac{1}{R\delta} = \frac{1}{l}\frac{1}{1 + K_{us}\frac{V^2}{gl}}, \tag{B.54}$$

where

$$K_{us} = \frac{mg}{l^2}\left(\frac{b}{C_1} - \frac{a}{C_2}\right) \tag{B.55}$$

is the so-called *understeer coefficient* or *understeer gradient* of the vehicle. The understeer coefficient is a non-dimensional quantity, and is often expressed in radians.

As already stated, in kinematic conditions

$$\left(\frac{1}{R\delta}\right)_{\text{kin}} = \frac{1}{l}. \tag{B.56}$$

The expression $1 + K_{us}V^2/gl$ can be considered as a correction factor giving the response of the vehicle in dynamic conditions as opposed to kinematic conditions.

From Eq. (B.53) it follows that

$$\delta - \delta_{\text{kin}} = \frac{V^2}{Rg}K_{us}, \tag{B.57}$$

i.e.,

$$K_{us} = \frac{g}{a_y}\left(\delta - \delta_{\text{kin}}\right). \tag{B.58}$$

The understeer factor can thus be interpreted as the difference between the steering angles in kinematic and dynamic conditions divided by the centrifugal acceleration expressed as a multiple of the gravitational acceleration.

Sometimes, instead of the understeer coefficient, a *stability factor*

$$K = \frac{m}{l^2}\left(\frac{b}{C_1} - \frac{a}{C_2}\right) \tag{B.59}$$

is defined.

As a first approximation, K and K_{us} may be considered as constants for a given vehicle and load condition. However, their dependence on speed cannot be neglected for more precise assessments.

It is possible to define a *lateral acceleration* gain as the ratio between the lateral acceleration and the steering input:

$$\frac{V^2}{R\delta} = \frac{V^2}{l}\frac{1}{1 + K_{us}\frac{V^2}{gl}}. \tag{B.60}$$

The sideslip angle can be obtained through simple geometrical considerations, yielding

$$\beta = \frac{b}{R} - \alpha_2. \tag{B.61}$$

A *sideslip angle gain* , expressing the ratio between the sideslip angle and the steering angle can be defined as well. Its value is

$$\frac{\beta}{\delta} = \frac{b}{l}\left(1 - \frac{maV^2}{blC_2}\right)\frac{1}{1 + K_{us}\frac{V^2}{gl}}, \tag{B.62}$$

B.4.4 Definition of Understeer and Oversteer

If $K_{us} = 0$ the value of $1/R\delta$ is constant and equal to the value characterizing kinematic steering; i.e. the response of the vehicle to a steering input is, at any speed, equal to that in kinematic conditions. This does not mean, however, that the vehicle is in kinematic conditions, since the value of the sideslip angle β is not equal to its kinematic value and the values of the sideslip angles of the wheels are not equal to zero.

A vehicle behaving in this way is said to be *neutral-steer* (Fig. B.9a).

If $K_{us} > 0$ the value of $1/R\delta$ decreases with increasing speed. The response of the vehicle is thus smaller than in kinematic conditions and, to maintain a constant radius of the path, the steering angle must be increased as the speed increases. A vehicle behaving in this way is said to be *understeer* .

A quantitative measure of the understeer of a vehicle is given by the *characteristic speed*, defined as the speed at which the steering angle needed to negotiate a turn is equal to twice the Ackerman angle, i.e. the path curvature gain is equal to $1/2l$.

Using the simplified approach outlined above, the characteristic speed is

$$V_{car} = \sqrt{\frac{gl}{K_{us}}} = \sqrt{\frac{1}{K}}. \tag{B.63}$$

If $K_{us} < 0$ the value of $1/R\delta$ increases with increasing speed until, for a speed

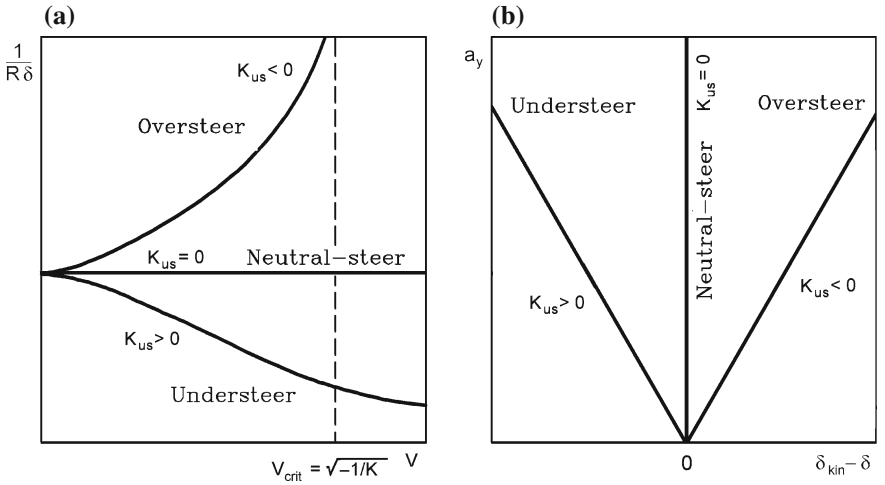

Fig. B.9 Steady state response to a steering input. Plot of the path curvature gain as a function of speed (**a**) and handling diagram (**b**) for an oversteer, an understeer and a neutral steer vehicle. The understeer factor is assumed to be independent of speed

$$V_{crit} = \sqrt{-\frac{gl}{K_{us}}} = \sqrt{-\frac{1}{K}} \tag{B.64}$$

the response tends to infinity, i.e., the system develops an unstable behavior.

A vehicle behaving in this way is said to be *oversteer* , and the speed given by Eq. (B.64) is called the *critical speed*. The critical speed of any oversteer vehicle must be well above the maximum speed it can reach, at least in normal road conditions.

Instead of plotting the path curvature gain as a function of the speed, it is possible to plot the *handling diagram*, i.e., the plot of the lateral acceleration a_y as a function of $\delta_{\text{kin}} - \delta$ (Fig. B.9b). If the vehicle is neutral steer, the plot is a vertical straight line, if it is oversteer it is a straight line sloping to the right, while in case of an understeer vehicle it slopes to the left.

The value of β, or better, of β/δ, decreases with the speed from the kinematic value up to the speed

$$(V)_{\beta=0} = \sqrt{\frac{blC_2}{am}} \tag{B.65}$$

at which it vanishes. At higher speed it becomes negative, tending to infinity when approaching the critical speed for oversteer vehicles and tending to

$$\frac{aC_1}{aC_1 - bC_2}$$

when the speed tends to infinity in the case of understeer vehicles.

B.4.5 High-Speed Cornering

The study of handling seen in the previous sections was based on the assumption of steady-state operation. Moreover, only the cornering forces acting on the tires were considered.

A simple mathematical model for the handling behavior of a rigid vehicle that overcomes the above limitations can, however, be built. The vehicle is considered as a rigid body moving on a surface, and thus a model with three degrees of freedom is needed for the study of its motion. If the road is considered as a flat surface, the motion is planar. By using the inertial reference frame[9] XY shown in Fig. B.10, it is possible to use the coordinates X and Y of the centre of mass G of the vehicle and the yaw angle ψ between the x and X axes as generalized coordinates.

To keep the model as simple as possible, the sideslip angle of the vehicle β and of the wheels α_i are small. The yaw angular velocity $\dot{\psi}$ is also considered as a small quantity.

The equations of motion of the vehicle are

$$\begin{cases} m\ddot{X} = F_X \\ m\ddot{Y} = F_Y \\ J_z\ddot{\psi} = M_z, \end{cases} \tag{B.66}$$

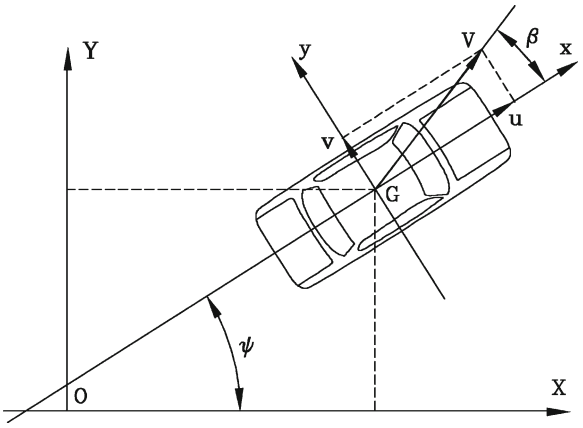

Fig. B.10 Reference frame for the study of the motion of a rigid vehicle. The vehicle has three degrees of freedom, and the coordinates X and Y of the centre of mass G and the yaw angle ψ can be used as generalized coordinates

[9] As already stated, such a reference frame is not, strictly speaking, inertial, since it is fixed to the road surface and hence follows the motion of Earth. It is, however, inertial "enough" for the problems here studied, and this issue will not be dealt with any further.

where F_X, F_Y and M_z are the total forces acting in the X and Y directions and the total yaw moment. Equation (B.66) are very simple but include the forces acting on the vehicle in the direction of the axes of the inertial frame. They are clearly linked with the forces acting in the directions of axes x and y of the vehicle by the obvious relationship

$$\left\{ \begin{array}{c} F_X \\ F_Y \end{array} \right\} = \left[\begin{array}{cc} \cos(\psi) & -\sin(\psi) \\ \sin(\psi) & \cos(\psi) \end{array} \right] \left\{ \begin{array}{c} F_x \\ F_y \end{array} \right\}. \tag{B.67}$$

If the model is used to perform a numerical integration in time, they can be used directly without any difficulty.

However, if the model has to be used to obtain linearized equations to gain a general insight into the behavior of the vehicle, it is better to write the equations of motion with reference to the non-inertial xy frame, to avoid dealing with the trigonometric functions of angle ψ, which in general is not a small angle, and would make linearizations impossible.

To write the equations of motion with reference to the body-fixed frame xyz , it is expedient to use the components u and v of the speed in the directions of the x and y axes and the yaw angular velocity

$$r = \dot{\psi}.$$

There are many ways to obtain the mathematical model, but perhaps the simplest is to remember that the derivative with respect to time of a generic vector $\vec{A}$, expressed in the body-fixed frame, but performed in the inertial frame

$$\left. \frac{d\vec{A}}{dt} \right|_i,$$

can be expressed starting from the derivative performed in the body fixed frame

$$\left. \frac{d\vec{A}}{dt} \right|_m$$

as

$$\left. \frac{d\vec{A}}{dt} \right|_i = \left. \frac{d\vec{A}}{dt} \right|_m + \vec{\Omega} \wedge \vec{A}, \tag{B.68}$$

where $\vec{\Omega}$ is the absolute angular velocity of the body-fixed frame.

Remembering that the velocity V is contained in the xy plane,

$$\left. \frac{d\vec{V}}{dt} \right|_m + \vec{\Omega} \wedge \vec{V} = \left\{ \begin{array}{c} \dot{u} - rv \\ \dot{v} + ru \\ 0 \end{array} \right\}, \tag{B.69}$$

the equations of motion of the vehicle, expressed with reference to the xyz frame, are thus

$$\begin{cases} m(\dot{u} - rv) = F_x \\ m(\dot{v} + ru) = F_y \\ J_z\dot{r} = M_z. \end{cases} \tag{B.70}$$

Equation (B.70) are nonlinear in the velocities u, v and r but, since the sideslip angle β is small and its trigonometric functions can be linearized, the linearization of the equations is possible. The components of velocity V can be written as

$$\begin{cases} u = V\cos(\beta) \approx V \\ v = V\sin(\beta) \approx V\beta. \end{cases} \tag{B.71}$$

Product $\dot{\psi}v$ can be considered the product of two small quantities and it is thus of the same order as the first term ignored in the series for the cosine. It is therefore cancelled.

The speed V can be considered as a known function of time, which amounts to studying the motion with a given law $V(t)$ (in many cases at constant speed) and assuming as an unknown the driving or the braking force needed to follow such a law. The unknown for the degree of freedom related to translation along the x-axis in this case is the force F_{x_d} exerted by the driving wheels. When braking, force F_x is the total braking force exerted by all wheels.

Equation (B.70) reduces to the linear form in F_x, v and r:

$$\begin{cases} m\dot{V} = F_x \\ m\,(\dot{v} + rV) = F_y\,. \\ J_z\dot{r} = M_z \end{cases} \tag{B.72}$$

If the interaction between longitudinal and transversal forces due to the tires is neglected or accounted for in an approximate way, the first equation of motion, which has already been studied in the section dealing with the longitudinal performance of the vehicle, uncouples from the other two.

This amounts to saying that the lateral behavior is uncoupled from the longitudinal behavior and can be studied using just two variables, either velocities v and r:

$$\begin{cases} m\,(\dot{v} + rV) = F_y \\ J_z\dot{r} = M_z \end{cases}, \tag{B.73}$$

or β and r if the equations are written in the equivalent form

$$\begin{cases} mV\left(\dot{\beta} + r\right) + m\beta\dot{V} = F_y \\ J_z\dot{r} = M_z \end{cases}. \tag{B.74}$$

The sideslip angles of the wheels may be expressed easily in terms of the generalized velocities. With simple computations it follows that

$$\alpha_i = \arctan\left(\frac{v + \dot{\psi} x_i}{u - \dot{\psi} y_i}\right) - \delta_i \tag{B.75}$$

where x_i and y_i are the coordinates of the center of the contact area of the ith wheel in the reference frame of the vehicle.

Equation (B.75) can be easily linearized. By noting that $y_i \dot{\psi}$ is far smaller than the speed V, it follows that

$$\alpha_i = \beta_i - \delta_i \approx \frac{v + r x_i}{V} - \delta_i = \beta + \frac{x_i}{V} r - \delta_i. \tag{B.76}$$

Coordinate y_i of the centre of the contact area of the wheel does not appear in the expression for the sideslip angle α_i. If the differences between the steering angles δ_i of the wheels of the same axle are neglected, the values of their sideslip angles are equal. This allows one to work in terms of axles instead of single wheels and to substitute a model of the type of Fig. B.6b for that of Fig. B.6a, i.e. to use a monotrack or bicycle model.

The explicit expressions of the sideslip angles of the front and rear axles of a vehicle with two axles are thus

$$\begin{cases} \alpha_1 = \beta + \dfrac{a}{V} r - \delta_1 \\ \\ \alpha_2 = \beta - \dfrac{b}{V} r - \delta_2 \end{cases}. \tag{B.77}$$

In the majority of cases only the front axle can steer and $\delta_2 = 0$.

The total lateral force is a function of the sideslip angle β and the yaw velocity r, which can be considered as the variables of the motion, and the steering angle δ, which can be considered as the control variable. By developing in Taylor series the force $F_y(\beta, r, \delta)$ about the condition $\beta = r = \delta = 0$, and truncating it after the linear term, it follows that

$$F_y = Y_\beta \beta + Y_r r + Y_\delta \delta + F_{y_e}, \tag{B.78}$$

where coefficients Y_β, Y_r and Y_δ are the derivatives of the force with respect to the three variables β, r and δ and may be obtained in any way, even experimentally, if possible. They are called the derivatives of stability of the vehicle.

In the same way, the linearized expression for the yawing moments is

$$M_z = N_\beta \beta + N_r r + N_\delta \delta + M_{z_e}, \tag{B.79}$$

where N_β, N_r and N_δ are other derivatives of stability of the vehicle. F_{y_e} and M_{z_e} are external forces and moments acting on the vehicle and can be considered as disturbances.

Equation (B.74) can be written directly as a state equation

$$\dot{\mathbf{z}} = \mathbf{A}\mathbf{z} + \mathbf{B}_c\mathbf{u}_c + \mathbf{B}_e\mathbf{u}_e, \tag{B.80}$$

where the state and input vectors $\mathbf{z}$, $\mathbf{u}_c$ and $\mathbf{u}_e$ are

$$\mathbf{z} = \begin{Bmatrix} \beta \\ r \end{Bmatrix}, \qquad \mathbf{u}_c = \delta, \qquad \mathbf{u}_e = \begin{Bmatrix} F_{y_e} \\ M_{z_e} \end{Bmatrix},$$

the dynamic matrix is

$$\mathbf{A} = \begin{bmatrix} \dfrac{Y_\beta}{mV} - \dfrac{\dot{V}}{V} & \dfrac{Y_r}{mV} - 1 \\ \dfrac{N_\beta}{J_z} & \dfrac{N_r}{J_z} \end{bmatrix}$$

and the input gain matrices are

$$\mathbf{B}_c = \begin{bmatrix} \dfrac{Y_\delta}{mV} \\ \dfrac{N_\delta}{J_z} \end{bmatrix}, \; \mathbf{B}_e = \begin{bmatrix} \dfrac{1}{mV} & 0 \\ 0 & \dfrac{1}{J_z} \end{bmatrix}.$$

The study of the system is straightforward: The eigenvalues of the dynamic matrix allow one to see immediately whether the behavior is stable or not, and the study of the solution to given constant inputs yields the steady state response to a steering input or to external forces and moments.

B.5 Vertical Dynamics (Comfort)

In all motor vehicles, with the exception of a few slow industrial vehicles, the wheels are connected to the chassis through elements provided with elasticity and damping: the suspensions. Their aim is to:

- Provide that the forces exchanged by the wheels with the ground comply with design specifications in every load condition;
- determine the vehicle *trim* under the action of static and quasi static forces;
- absorb and smooth down shocks that are received by the wheels from road irregularities and transmitted to the body.

Owing to the presence of the suspensions, the vehicle body, that is usually assumed to be a rigid body, can move in a direction perpendicular to the ground (z-axis in Fig. B.1, heave motion) and can rotate about x -axis (roll motion) and about y-axis (pitch motion). The vehicle is thus assumed to be composed by a *sprung mass*, coinciding with the body, plus a number of *unsprung masses*, each containing a wheel and some mechanical components.

If the assumptions of symmetry and linearity mentioned in Sect. B.1 hold, the heave and pitch motions are coupled with each other, while roll motion uncouples or, better, roll motion couples with the handling behavior of the vehicle.

B.5.1 Heave and Pitch Motion

In the study of the low frequency motion of the sprung mass, the tires can be considered as rigid bodies, i.e. the unsprung masses can be assumed as rigidly connected with the ground. The simplest model for studying the heave-pitch coupling is shown in Fig. B.11a. Its equation of motion is that of a beam on two elastic and damped supports

$$\begin{bmatrix} m_S & 0 \\ 0 & J_y \end{bmatrix} \begin{Bmatrix} \ddot{Z}_s \\ \ddot{\theta} \end{Bmatrix} + \begin{bmatrix} c_1 + c_2 & -ac_1 + bc_2 \\ -ac_1 + bc_2 & a^2 c_1 + b^2 c_2 \end{bmatrix} \begin{Bmatrix} \dot{Z}_s \\ \dot{\theta} \end{Bmatrix} +$$

$$+ \begin{bmatrix} K_1 + K_2 & -aK_1 + bK_2 \\ -aK_1 + bK_2 & a^2 K_1 + b^2 K_2 \end{bmatrix} \begin{Bmatrix} Z_s \\ \theta \end{Bmatrix} = \tag{B.81}$$

$$= \begin{Bmatrix} c_1 \dot{h}_A + c_2 \dot{h}_B + K_1 h_A + K_2 h_B \\ -ac_1 \dot{h}_A + bc_2 \dot{h}_B - aK_1 h_A + bK_2 h_B \end{Bmatrix}$$

where h_A and h_B are the z coordinate of the centers of the wheels, that under the assumption of rigid tires coincide, except for a constant, with the z coordinate of the wheel-ground contact points. They thus define the ground profile, or better, the average between the ground profiles under the right and left wheels.

The overturning moment due to weight (term $-m_S g h$ to be added in position 22 in the stiffness matrix) is not included in Eq. (B.81), because no assumption has been made on the height of the pitch center over the road plane, nor is any aerodynamic term introduced into the equation of motion. The longitudinal position of the springs and the shock absorbers has been assumed to be the same.

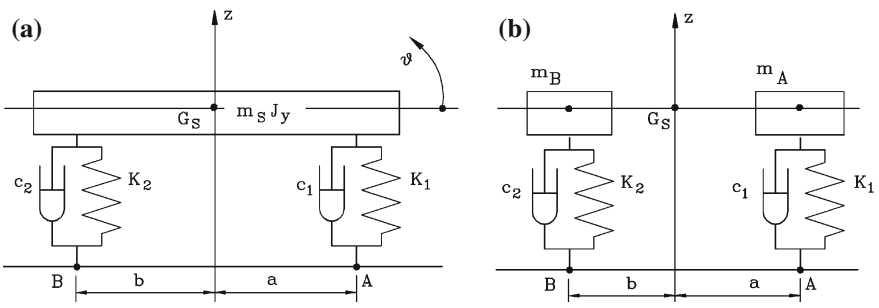

Fig. B.11 Beam models for heave and pitch motions

The forcing functions were written in a form that considers only the vertical motion of points A and B, neglecting horizontal forces at the ground-wheels interface and the possible coupling between vertical and horizontal motions due to suspensions.

If mass m_s and moment of inertia J_y are those of the whole sprung mass, the stiffnesses K_i and the damping coefficients c_i are those of a whole axle and are thus twice those of a single spring or shock absorber.

A *dynamic index* I_d of the sprung mass can be defined as

$$I_d = \frac{J_y}{m_s ab} = \frac{r_y^2}{ab}, \tag{B.82}$$

where r_y is the radius of gyration of the sprung mass. If I_d is equal to unity, i.e. if

$$J_y = m_S ab, \quad r_y^2 = ab,$$

the model of Fig. B.11a reduces to that of Fig. B.11b, i.e. the motion of the sprung mass reduce to the motion of two masses

$$m_A = m_S \frac{b}{l} \text{ and } m_B = m_S \frac{a}{l},$$

suspended on the front and rear suspensions.

This condition is usually not verified in practice. The tendency to increase the wheelbase for stability reasons leads to values of the dynamic index usually smaller than 1, even smaller than 0.8.

The natural frequencies of the undamped system may be computed using the homogeneous equation associated with Eq. (B.81), after cancelling the damping term. They are thus the roots of the characteristic equation

$$\omega^4 - \omega^2 \frac{K_1(r_y^2 + a^2) + K_2(r_y^2 + b^2)}{m_S r_y^2} + K_1 K_2 \frac{l^2}{m_S^2 r_y^2} = 0, \tag{B.83}$$

that yields

$$\omega_i = \frac{\sqrt{\left(b^2 + r_y^2\right) K_2 + \left(a^2 + r_y^2\right) K_1 \pm \Delta}}{r_y \sqrt{2 m_S}}, \tag{B.84}$$

where

$$\Delta = \sqrt{\left(b^2 + r_y^2\right)^2 {K_2}^2 + 2 K_1 K_2 \left[\left(ab - r_y^2\right)^2 - r_y^2 l^2\right] + \left(a^2 + r_y^2\right)^2 {K_1}^2}\,.$$

The solution with the (+) sign yields two positive values, that generally are not equal to each other. The motion of the beam is neither a rotation about its center of

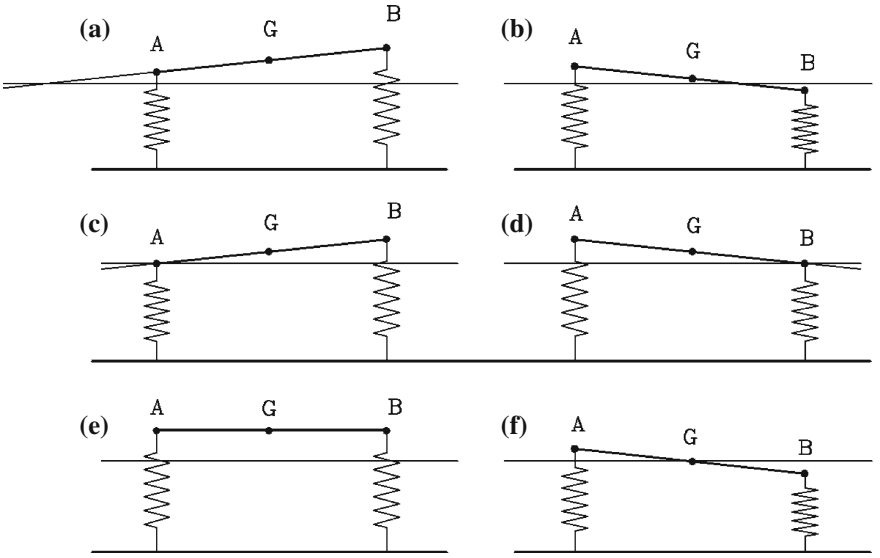

Fig. B.12 Heave and pitching motions. **a** and **b**: General case; primarily heave (**a**) and primarily pitching (**b**) motions. **c** and **d**: Case with $I_d = 1$. **e** and **f**: Case with $aK_1 = bK_2$.

mass (pitch) nor a translational motion in the z direction (heave), but the very fact that the displacements at the front and rear axles have the same sign means that the node (the point with zero displacement) lies outside of the wheelbase, and thus the motion is primarily translational (heave, Fig. B.12a). The solution with the $(-)$ sign (Fig. B.12b) yields a positive and a negative value: the displacements of the front and rear axles are one positive and one negative and the node is within the wheelbase. The motion is primarily rotational, even if not about the center of mass, and it is primarily a pitching motion.

If the dynamic index I_d has a unit value (Fig. B.12c, d), it follows that

$$\omega_1 = \sqrt{\frac{lK_2}{am_S}}, \quad \omega_2 = \sqrt{\frac{lK_1}{bm_S}}. \tag{B.85}$$

As previously stated, the natural frequencies in this case are those of the two separate masses of Fig. B.11b and the free oscillations of the sprung mass are rotations about the points where the suspensions are connected to the body. It is impossible to identify a heave and a pitch mode; it is more accurate to speak about a front-axle and a rear-axle mode.

The other limiting case (Fig. B.12e, f) is when

$$aK_1 = bK_2. \tag{B.86}$$

The heave motion uncouples from the pitch motion. The first is translational, while the second is rotational and occurs about the center of mass. The natural frequencies are thus

$$\begin{cases} \omega_1 = \sqrt{\dfrac{lK_1}{bm_S}} & \text{heave,} \\ \omega_2 = \sqrt{\dfrac{laK_1}{r_y^2 m_S}} = \omega_1 \sqrt{\dfrac{ab}{r_y^2}} & \text{pitch.} \end{cases} \tag{B.87}$$

The two limiting cases may also occur simultaneously. From Eq. (B.87) it follows that when this is the case the two natural frequencies have the same value. This solves an apparent inconsistency; if

$$aK_1 = bK_2,$$

the centers of rotation are one in the centre of mass (pitch mode) and one at infinity (heave mode), while when the dynamic index has a unit value they are at the ends of the wheelbase. When both conditions occur simultaneously, the two natural frequencies coincide; in this case, any linear combination of the eigenvectors is itself an eigenvector. Thus in the case of a rigid beam, any point of the beam (or better, of the straight line constituting the beam axis) may be considered as a center of rotation.

In the study of high frequency motions, the compliance of tires cannot be neglected, and the model must contain also the unsprung masses. The minimum number of degrees of freedom needed to study heave and pitch motions is thus four.

B.5.2 Quarter-Car Models

The simplest model for studying the suspension motions of a vehicle is the so-called *quarter-car model* , including a single wheel with the related suspension and the part of the body whose weight is imposed on it. Often, in four-wheeled vehicles, the quarter vehicle including the suspension and the wheels is called a *corner* of the vehicle. The quarter-car model may be more or less complex, including not only the compliance of the suspension, but also the compliance of the tire and that of the rubber mounts connecting the frame carrying the suspension to the body. It may even include the inertia of the tire.

Three models based on the quarter-car approach are shown in Fig. B.13.

The first model has a single degree of freedom. The tires are considered rigid bodies and the only mass considered is the sprung mass. This model holds well for motions taking place at low frequency, in the range of the natural frequency of the sprung mass (in most cases, up to 3–5 Hz, in the range defined as *ride* by SAE).

The second model has two degrees of freedom. The tire is considered as a massless spring, and both the unsprung and the sprung masses are considered. This model holds well for frequencies up to the natural frequency of the unsprung mass and slightly

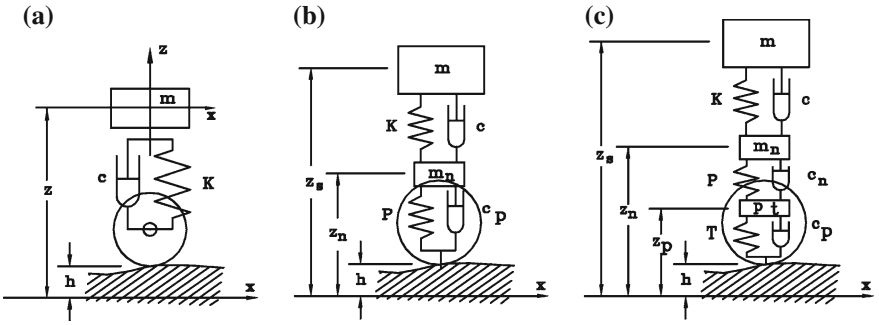

Fig. B.13 Quarter-car models with one (**a**), two (**b**) and three (**c**) degrees of freedom

over (in most cases, up to 30–50 Hz, including the ranges defined as *ride*, *shake* and partially *harshness*).

The third model has three degrees of freedom. The tire is modelled as a spring-mass-damper system, representing its dynamic characteristics in the lowest mode. This model allows us to study motions taking place at frequencies in excess of the first natural frequency of the tires (up to $120 - 150$ Hz, including *harshness*).

If higher frequencies must be accounted for, it is possible to introduce a higher number of tire modes by inserting other masses. These models, essentially based on the modal analysis of the suspension-tire system, are clearly approximated because a tire can be considered as a damped system and one that is usually nonlinear.

Consider the simplest quarter-car model shown in Fig. B.13a. It is a simple mass-spring-damper system that, among other things, has been used in the past to demonstrate that the shock absorber must be a linear, symmetrical viscous damper.[10]

The equation of motion of the system is simple. Using the symbols shown in the figure it is

$$m\ddot{z} + c\dot{z} + Kz = c\dot{h} + Kh, \tag{B.88}$$

where $z\,(t)$ is the displacement from the static equilibrium position, referred to an inertial frame, and $h\,(t)$ is the vertical displacement of the supporting point due to road irregularities.[11]

The frequency response of the quarter-car can be obtained simply by stating a harmonic input of the type

$$h = h_0 e^{i\omega t}.$$

The output is itself harmonic and can be expressed as

[10] Bourcier De Carbon C.: *Théorie mathématiques et ré alisation pratique de la suspension amortie des vehicules terrestres*, Proceedings SIA Conference, Paris, 1950.

[11] The z coordinate must be considered as the displacement from the static equilibrium position. By doing this, the static problem of finding the equilibrium position is separated from the dynamic problem here dealt with. This can only be done because of the linearity of the model.

$$z = z_0 e^{i\omega t},$$

where both amplitudes h_0 and z_0 are complex numbers to account for the different phasing of response and excitation due to damping.

By introducing the time histories of the forcing function and of the response into the equation of motion, an algebraic equation is obtained:

$$\left(-\omega^2 m + i\omega c + K\right) z_0 = (i\omega c + K)\, h_0. \tag{B.89}$$

It links the amplitude of the response to that of the excitation, and yields

$$z_0 = h_0 \frac{i\omega c + K}{-\omega^2 m + i\omega c + K}. \tag{B.90}$$

If h_0 is real (that is, if the equation is written in phase with the excitation), the real part of the response (the in-phase component of the response) can be separated easily from its imaginary part (in-quadrature component)

$$\begin{cases} \dfrac{Re\,(z_0)}{h_0} = \dfrac{K\left(K - m\omega^2\right) + c^2\omega^2}{\left(K - m\omega^2\right)^2 + c^2\omega^2} \\ \dfrac{Im\,(z_0)}{h_0} = \dfrac{-cm\omega^3}{\left(K - m\omega^2\right)^2 + c^2\omega^2}. \end{cases} \tag{B.91}$$

The amplification factor, i.e., the ratio between the absolute values of the amplitudes of the response and the excitation and the phase of the first with respect to the second, can be easily shown to be (Figs. B.14a, c)

$$\begin{cases} \dfrac{|z_0|}{|h_0|} = \sqrt{\dfrac{K^2 + c^2\omega^2}{\left(K - m\omega^2\right)^2 + c^2\omega^2}} \\ \Phi = \arctan\left(\dfrac{-cm\omega^3}{K\left(K - m\omega^2\right) + c^2\omega^2}\right). \end{cases} \tag{B.92}$$

More than the frequency response expressing the ratio between the amplitudes of response and excitation, what matters in motor vehicle suspensions is the ratio between the amplitudes of the acceleration of the sprung mass and that of the displacement of the supporting point. Because in harmonic motion the amplitude of the acceleration is equal to the amplitude of the displacement multiplied by the square of the frequency, it follows that:

$$\frac{|(\ddot{z})_0|}{|h_0|} = \omega^2 \frac{|z_0|}{|h_0|}.$$

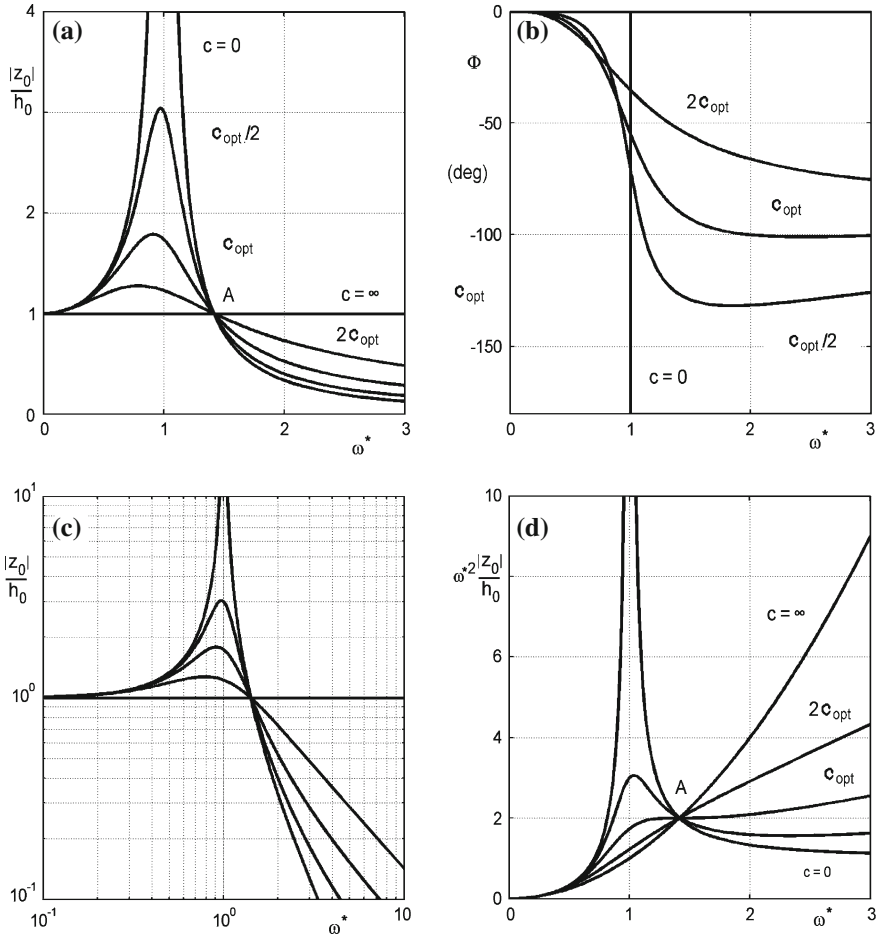

Fig. B.14 Quarter-car with a single degree of freedom, response to harmonic excitation. **a** and **b** Ratio between the amplitude of the response (in terms of displacement, linear scale) and the amplitude of the ground displacement, and phase as functions of the non-dimensional frequency $\omega^* = \omega\sqrt{m/K}$. **c** Same as **a**, but plotted in a logarithmic scale. **d** Same as **a**, but for the acceleration of the sprung mass

Both frequency responses are plotted in Fig. B.14 for different values of the damping of the shock absorber, together with the phase Φ . The responses are plotted as functions of the nondimensional frequency

$$\omega^* = \omega\sqrt{\frac{m}{K}}$$

and damping is expressed as a function of the optimum damping defined below.

All curves pass through point A, located at a frequency equal to $\sqrt{2K/m}$. Because the acceleration of the sprung mass must be kept to a minimum to produce a comfortable ride, a reasonable way to optimize the suspension is to choose a value of shock absorber damping that leads to a relative maximum, or at least a stationary point, at point A on the curve related to acceleration. By differentiating the expression of

$$\omega^2 \frac{|z_0|}{|h_0|}$$

with respect to ω and equating the derivative to zero at point A, the following value of the optimum damping is obtained:

$$c_{opt} = \sqrt{\frac{Km}{2}} = \frac{c_{cr}}{2\sqrt{2}}, \tag{B.93}$$

where

$$c_{cr} = 2\sqrt{Km}$$

is the critical damping of the suspension .

Although this method for optimizing the suspension can be readily criticized, because the comfort of a suspension is far more complex than simple reduction of the vertical acceleration (the so-called "jerk", i.e., the derivative of the acceleration with respect to time d^3z/dt^3 also plays an important role), it nonetheless gives important indications.

The dynamic component of the force the tire exerts on the ground is

$$F_z = c\left(\dot{z} - \dot{h}\right) + K(z - h) = -m\ddot{z}. \tag{B.94}$$

Minimizing the vertical acceleration leads to minimizing the dynamic component of the vertical load on the tire, which has a negative influence on the ability of the tire to exert cornering forces. The condition leading to optimum comfort seems, thus, to coincide with that leading to optimum handling performance. Equation (B.93) allows one to choose the value of the damping coefficient c. For the value of the stiffness K there is no such optimization: To minimize both the acceleration and the dynamic component of the force, K should be kept as low as possible. The only limit to the softness of the springs is the space available.

This reasoning has, however, the following limitation: The softer the springs, the larger the oscillations of the sprung mass. Large displacements must be avoided because they may cause large errors in the working angles of the tire, causing the tires to work in conditions that may be far from optimal.

An empirical rule states that soft suspensions improve comfort while hard suspensions improve handling. This is even more true if aerodynamic devices are used to produce negative lift: suspensions allowing a large degree of travel cause major changes of vehicle position with respect to the airflow, producing changes of the aerodynamic lift that are detrimental.

Moreover, at a fixed value of the sprung mass, the lower the stiffness of the spring, the lower the natural frequency. Very soft suspensions easily lead to natural frequencies of about 1 Hz or even less, which may cause motion sickness and a reduction in comfort that varies from person to person. Cars with soft suspensions with large travel, typical of some manufacturers, are popular with some customers but considered uncomfortable by others.

The optimum value of the damping expressed by Eq. (B.93) is lower than the critical damping. The quarter-car is then underdamped and may undergo free oscillations, even if these generally damp out quickly because the damping ratio $\zeta = c/c_{cr}$ is not very low:

$$\frac{c_{opt}}{c_{cr}} = \frac{1}{2\sqrt{2}} \approx 0.354. \tag{B.95}$$

As for the previous case, when studying higher frequency motions, the compliance of the tires must be accounted for and more complex quarter car models must be used.

B.5.3 Roll Motion

As already stated, roll is coupled with handling and not with ride comfort. However it is also true that rolling can affect strongly the subjective feeling of riding comfort.

The simplest model for studying roll motion is made by a rigid body, simulating the sprung mass, free to rotate about the roll axis, constrained to the ground by a set of springs and dampers with a stiffness and a damping coefficient equal to those of the suspensions (Fig. B.15). If J_x, m_s, χ_i and Γ_i are respectively the moment of inertia about the roll axis, the sprung mass, the torsional stiffness and the damping coefficient of the ith suspension, the equation of motion is

$$J_x\ddot{\phi} + (\Gamma_1 + \Gamma_2)\,\dot{\phi} + (\chi_1 + \chi_2)\,\phi - m_s g h_G \sin(\phi) = \tag{B.96}$$

$$= \Gamma_1\dot{\alpha}_{t_1} + \Gamma_2\dot{\alpha}_{t_2} + \chi_1\alpha_{t_1} + \chi_2\alpha_{t_2},$$

where the forcing functions are those due to the transversal inclination of the road α_{t_i} at the ith suspension.

The inertia of the unsprung masses and the compliance of the tires are not included in such a simple model, which is formally identical to the quarter-car with a single degree of freedom.

For small values of the roll angle, the model may be linearized, stating $\sin(\phi) \approx \phi$. The roll natural frequency is thus

$$\omega_{roll} = \sqrt{\frac{\chi_1 + \chi_2 - m_s g h_G}{J_x}}. \tag{B.97}$$

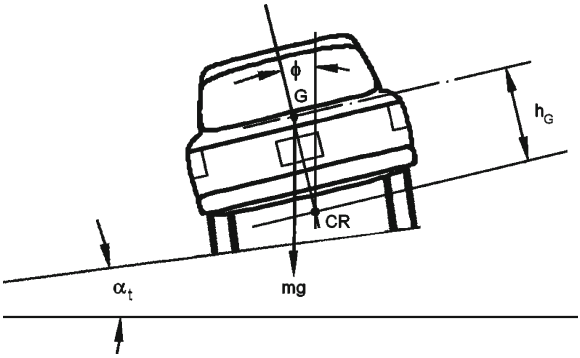

Fig. B.15 Model with a single degree of freedom for the study of roll motion. Cross section in a plane containing the center of mass G of the sprung mass. The roll axis goes through point CR

The optimum damping value may be obtained from Eq. (B.93):

$$\Gamma_{opt} = \sqrt{\frac{J_x\,(\chi_1 + \chi_2 - m_s g h_G)}{2}}. \tag{B.98}$$

This condition is generally not satisfied, particularly if the vehicle has anti-roll bars. The torsional damping of the suspensions is supplied by the same shock absorbers normally designed to optimize vertical motion; the roll damping they supply is usually lower than needed. The increase in stiffness due to anti-roll bars is not accompanied by an increase in damping, which causes a decrease of the damping ratio, together with an increase of the natural frequency.

The stiffer the suspension in torsion, the more underdamped the roll behavior, if the increase in stiffness is due to anti-roll bars. Although reducing rolling in stationary conditions, they may increase it in dynamic conditions. An overelongation in the step response, as when roll is due to a moment abruptly applied (steering step input, wind gusts or other similar instances), may then result. A large roll in dynamic conditions may cause rollover.

The stationary value of the roll angle on a road with transversal slope $\alpha_t = \alpha_{t_1} = \alpha_{t_2}$ is

$$\phi = \alpha_t \frac{\chi_1 + \chi_2}{\chi_1 + \chi_2 - m_s g h_G}. \tag{B.99}$$

The importance of a center of mass not too high on the roll axis and stiff suspensions (in roll) is thus clear. The last condition may contradict the need for a small roll in dynamic conditions.

B.6 Coupled Dynamics

When either the above mentioned assumptions do not hold, or the analyst wants to reach a higher precision, the whole vehicle must be modelled as a single system. A vehicle on elastic suspensions is usually modelled as a system made by a certain number of rigid bodies connected with each other by mechanisms of various kinds and by a set of massless springs and dampers simulating the suspensions. A vehicle with four wheels can be modelled as a system with 10 degrees of freedom, six for the body and one for each wheel. This holds for any type of suspension, if the motion of the wheels due to the compliance of the system constraining the motion of the suspensions (longitudinal and transversal compliance of the suspensions) is neglected. Additional degrees of freedom, such as the rotation of the wheels about their axis or about the kingpin, can be inserted into the model to allow the longitudinal slip or the compliance of the steering system to be taken into account.

The multibody approach can be pushed much further , by modelling, for instance, each of the links of the suspensions as a rigid body. To model a double wishbone suspension it is possible to resort to three rigid bodies, simulating the lower and upper triangles and the strut, plus a further rigid body simulating the steering bar. While modelling the system in greater detail, the number of rigid bodies included in the model increases. However, if the compliance of the various elements is neglected (i.e. if these bodies are rigid bodies), the number of degrees of freedom does not increase along with the number of bodies: a double wishbone suspension always has a single degree of freedom, even if it is made up of a number of rigid bodies simulating its various elements.

The mathematical model of a multibody system is thus made up of the equations of motion of the various elements, which in tridimensional space are $6n$, if n is the number of the rigid bodies, plus a suitable number of constraint equations.

Consider for instance an articulated truck with 6 solid axles (3 for the tractor plus 3 for the trailer). The rigid bodies are 8 (tractor, trailer and 6 rigid axles) and thus the equations of motion are 48 second-order differential equations. The constraint equations are 27: 3 equations for the constraint between tractor and trailer (these state that the coordinates of the center of the hitch, assumed to be a spherical hinge, are the same whether this point is seen as belonging to the tractor or to the trailer) and 4 equations for each axle, leaving to each one of them just two, out of its 6 degrees of freedom. The 27 constraint equations are algebraic equations containing only the generalized coordinates but not the velocities (holonomic constraints).

By using the 27 constraint equations to eliminate 27 of the generalized coordinates, a set of 21 equations in the 21 independent generalized coordinates is obtained. It must be emphasized that in the 48 equations of motion originally written, the forces the various bodies exchange at the constraints are included; these forces are then eliminated when the constraint equations are introduced. The 27 equations so eliminated can be used to compute the constraint forces.

This approach is the most general, and is usually implemented in *general purpose* multibody computer codes.

It is possible to resort to a simpler approach in the case of the multibody models used in motor vehicle dynamics, because the internal constraints are holonomic and the system is branched. One of the bodies (the vehicle's body) may be chosen as *main body*, to which a number of secondary, *first level* bodies are attached. Other secondary bodies, considered as *second level* bodies, are then attached, and so on. Secondary bodies have only the degrees of freedom allowed by the constraints. In this way, the minimum number of equations needed for the study are directly obtained. Such equations are all differential equations, usually of the second order. The forces exchanged at the constraints between the bodies do not appear explicitly in the equations and need not be computed in the dynamic study of the system as a whole. A model of the mentioned articulated truck with 6 solid axles can be obtained in this way: the tractor is considered as the main body, the axles of the tractor and the trailer are first level secondary bodies, and the axles of the trailer are second level secondary bodies.

The first approach is that followed by many commercial codes, like ADAMS, whose specialized version ADAMS-CAR is specifically adapted to automotive simulation. Some specialized commercial codes designed for motor vehicle simulation, like CarSim, are based on the second approach.

B.7 Symbols

a	Acceleration distance between centre of mass and front axle
b	Distance between centre of mass and rear axle
c	Viscous damping coefficient
c_{cr}	Critical damping
c_{opt}	Optimal damping
e	Energy
f	Rolling coefficient
f_0	Rolling coefficient at zero speed
g	Gravitational acceleration
i	Grade of the road
l	Wheelbase
m	Mass
m_e	Equivalent mass
q	Specific fuel consumption
r	Yaw velocity
t	Time; track
u, v, w	Velocities in the xyz frame
xyz	Body-fixed reference frame
$\mathbf{z}$	State vector
$\mathbf{A}$	Dynamic matrix in the state space
$\mathbf{B}$	Input gain matrix
C	Cornering stiffness
C_x, C_z	Aerodynamic coefficients
F	force
H	Thermal value of fuel
I_d	Dynamic index
J	Moment of inertia
K	Stiffness, stability factor, coefficient for the rolling resistance
P	Power
R	Radius of the wheel (unloaded); radius of the trajectory; resistance to motion
R_e	Effective rolling radius
S	Reference surface
$\mathcal{T}$	Kinetic energy
V	Vehicle speed
XYZ	Inertial frame
α	Sideslip angle; grade angle of the road
α_t	Transversal grade angle of the road
β	Sideslip angle of the vehicle
γ	Camber angle
δ	Steering angle
η	Efficiency

θ Pitch angle
μ_x Longitudinal force coefficient
μ_y Cornering force coefficient
ρ Density
τ Transmission ratio
ϕ Roll angle
χ Torsional stiffness
ψ Yaw angle
ω Frequency
ω_n Natural frequency
Γ Rotational damping coefficient
Φ Phase
Ω Angular velocity

References

—, *Diesel Engine Management, Robert Bosch GmbH* (Professional Engineering Publishing, Stuttgart, 2005)
—, Dinglers Politechnischer Journal, Band **310** (1898)
—, Dinglers Politechnischer Journal, Band **314** (1899)
—, Dinglers Politechnischer Journal, Band **315** (1900)
—, *Gasoline engine management, robert bosch GmbH* (Professional Engineering Publishing, Stuttgart, 2004)
—, *L'industria automobilistica mondiale 2000–2010*, (Anfia, Torino, 2010)
—, Progetto archivio storico FIAT, I primi quindici anni della FIAT, Franco Angeli (1987)
—, *The automobile, a century of progress* (SAE, Warrendale, 1997)
—, *The global automotive industry value chain* (UNIDO, Vienna, 2003)
D. Baker, B. Hammerle, R. Backes, *Urea infrastrucuture for control ov vehicular* NO_x *emissions* (Aachener Kolloquium Fahrzeug und Motorentechnik, Aachen, 2000)
P.L. Bassignana, *Storia fotografica dell'industria automobilistica italiana* (Bollati Boringhieri, Torino, 1998)
L. Baudry de Saunier, *L'automobile theorique e pratique*, 2 volumes (Omnia, Paris, 1900)
L. Baudry de Saunier, *L'allumage dans les moteurs a explosion* (Dunod, Paris, 1905)
C. Beatrice, C. Bertoli, M. Migliaccio, *Basic concepts of the homogeneous charge compression engines*, ATA Ingegneria dell'Autoveicolo, vol 55 (Torino, Turin, 2002)
L. Bernard, A. Ferrari, M. Ferrera, D. Micelli, Air Control and Direct Injection on Turbocharged Gasoline Engines, in *ATA Ingegneria dell'Autoveicolo*, vol 59 (2006)
G.P. Blair, *Design and simulation of four-stroke engines* (SAE International, Warrendale, 1999)
M. Boisseaux, *L'automobile méthodes de calcul* (Dunod, Paris, 1948)
E. Borchi, R. Macii, G. Ricci, I motori della scuola fiorentina, comitato manifestazioni 150° anniversario dell'invenzione del motore a scoppio (2003)
E. Borchi, R. Macii, G. Ricci, I padri del motore a scoppio, comitato manifestazioni 150° anniversario dell'invenzione del motore a scoppio (2003)
E.B. Butler, *Transmission gears* (Griffin, London, 1917)
C. Campbell, R. Bentley, *The sports car*, (Cambridge, 1954)
G. Canestrini, *L'automobile, il contributo italiano all'avvento e all'evoluzione dell'autoveicolo* (R.A.C.I., Kokomo, 1938)
F. Caputo, M. Martorelli, *Disegno e progettazione per la gestione industriale* (ESI, Napoli, 2003)
W.H. Crouse, *Automotive transmissions and power trains* (Mc Graw-Hill, New York, 1955)
C.L. Cummins, *Internal fire* (SAE, Warrendale, 1989)

G. Genta et al., *The Motor Car*, Mechanical Engineering Series,
DOI: 10.1007/978-94-007-8552-6, © Springer Science+Business Media Dordrecht 2014

W.F. Decker, *The story of the engine* (Scribner, London, 1932)
R. Devillers, P. Merces, *Le moteur a explosion* (Dunod, Paris, 1935)
V. Doria, A. Ferrari, M. Lucatello, U. Nasi, *The fiat uniair variable valve actuation system* (Variable valvetrain Conference, Essen, 2002)
C. Dugald, *The gas, petrol and oil engine* (Longmans, London, 1916)
E. Eckermann, *World history of the automobile* (SAE, Warrendale, 2001)
A. Eiser, Innovative technology for future powertrains, in *ATA Ingegneria dell'Autoveicolo*, vol 60 (2007)
R. Flieri, M. Klüting, *The third genaration of valvetrains: new fully variable valvetrains for throttle-free load control* (SAE Paper, Warrendale, 2000-01-1227)
G. Genta, L. Morello, *The automotive chassis*, 2 volumes (Springer, New York, 2009)
D. Giacosa, *Motori endotermici* (Hoepli, Milan, 1941)
D. Giacosa, *Progetti alla FIAT* (Automobilia, Torino, 1988)
B. Gille, Storia delle tecniche, Editori Riuniti (1985)
K.H. Glück, U. Göbel, H. Hahn, J. Höhne, R. Krebs, T. Kreuzer, E. Pott, *Die Abgasreinigung de FSI-Motoren von Volkswagen*, MTZ Motortechnische Zeitschrift (2000)
J. Gunn, *The practical design of motor cars* (Arnold, London, 1910)
J.B. Heywood, *Internal combustion engine fundamentals* (McGraw-Hill Book Company, New York, 1988)
A. Jamieson, E.S. Andrews, *Heat and heat engines* (Griffin and Co, Washington D.C., 1925)
R. Kaiser, K. Rusch, *Designing of SCR systems for reducing nitrogen oxide in diesel engines*, MTZ, Heft 12 (2007)
S. Kalpakjian, *Manufactring engineering and technology*, (Addison Wesley, Boston, 1989)
H. Klingenberg, D. Schürmann, *Unregulated motor vehicle exhaust gas components* (Volkswagen AG, Wolfsburg, 1989)
A. Levi Cases, *Atti del primo congresso del motore a scoppio* (Padova, 1927)
G. Lief, *The firestone story* (McGraw-Hill, New York, 1951)
J.C. Maroselli, *L'automobile et ses grands problèmes* (Larousse, Paris, 1958)
A. Mentasti, *Carrozzerie d'automobile* (Hoepli, Milano, 1929)
L. Morello, L. Rosti, G. Pia, A. Tonoli, *The automotive body*, 2 volumes (Springer, New York, 2011)
W. Neubecker, *Antique automobile body construction and restoration* (Post Publication, Arcadia, 1912)
J.P. Norbye, *Sports car suspension* (Sport Car Presse, New York, 1965)
G. Oliver, *Cars and coach building* (Sotheby Parke Bernet, London, 1981)
V.W. Page, *The modern gasoline automobile* (Hodder and Stoughton, London, 1917)
M. Peter, *Der Kraftwagen* (RC Schmidt, Berlin, 1937)
C. Riedl, *Konstruktion und berechnung moderner automobil- und kraftradmotoren* (Schmidt, Berlin, 1930)
G. Rogliatti, C. Valier, L. Giovanetti, *La frizione nel tempo* (Valeo, Torino, 1980)
C. Schmidt, *Practical Treatise on Automobiles* (The American Text-book, Philadelphia, 1909)
M. Schwaderlapp, Friction reduction: the mechanical contribution to fuel economy, in *ATA Ingegneria dell'Autoveicolo*, vol 61 (2008)
A. Seniga, *Il meccanismo di trasmissione negli automobili* (Biblioteca di automobilismo e aviazione, Milano, 1912)
M. Serruys, *La suspension et la direction des véhicules routiers* (Dunod, Paris, 1947)
F. Steinparzer, W. Mattes, P. Nefischer, T. Steinmayr, *Der Neue Vierzylinder-Dieselmotor von BMW*, MTZ, Heft 11 (2007)
J. Szybist, B. Bunting, Chemistry Impacs in Gasoline HCCI Engines, in *Literature Review for CRC Project AVFL-13* (Fuel Oak Ridge National Laboratory, 2006)
E. Tompkins, *The history of the pneumatic tyre*, Dunlop Archive Project (Eastland Press, London, 1981)

Index

G. Genta et al., *The Motor Car*, Mechanical Engineering Series,
DOI: 10.1007/978-94-007-8552-6, © Springer Science+Business Media Dordrecht 2014